Full-field coherent imaging of biological cells and tissues: high resolution, throughput and functional contrast

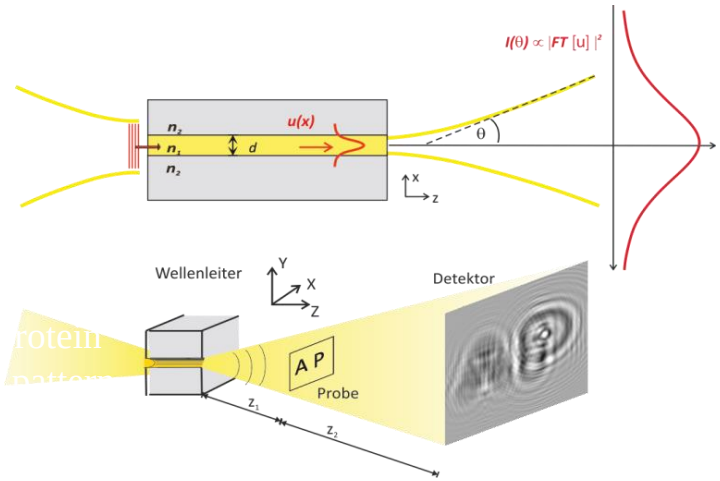

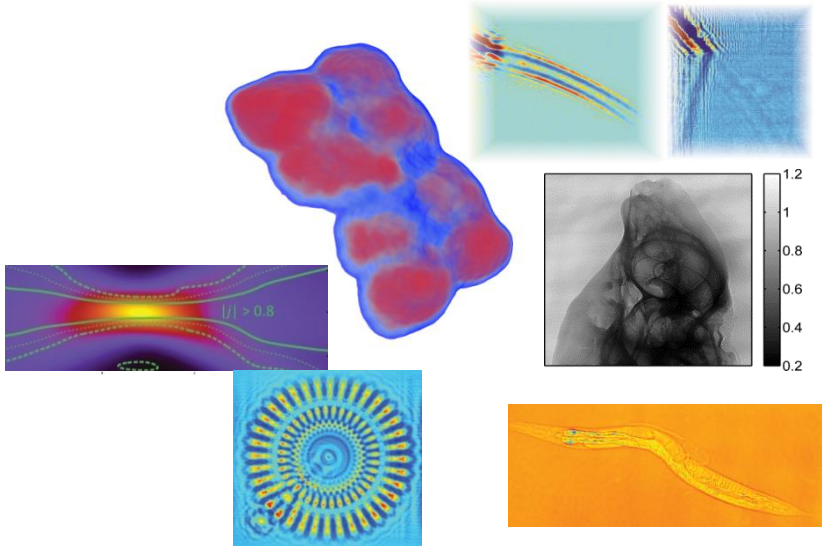

Tim Salditt

Institut für Röntgenphysik, Universität Göttingen,

Data Science Workshop, IMS NUS, 9.1.2018

SFB 755

1 7 3 7








Mareike Töpperwien *tomography of neural tissues*
Aike Ruhlandt *time-resolved tomography & 3d phase retrieval*
Malte Vassholz *waveguide optics & new tomography concepts*
Martin Krenkel *tomography of cells & tissues, waveguides, lab. CT*
Mathias Bartels *high resolution waveguide imaging, live cells, cochlea CT,*
Annalena Robisch *near-field ptychography*
Aike Ruhlandt *time-resolved tomography*

Johannes Hagemann
reconstruction
beyond idealisation

Markus Osterhoff *x-ray optics, numerics, GINIX endstation*

Sarah Hoffmann, *waveguide optics and fabrication*
Hsin-Yi Chen *tapered waveguides*
Robin Wilke, *phase reconstruction algorithms, ptychography*
Marten Bernhardt cellular imaging, stem cells, nano diffraction
Marius Priebe cellular imaging, action
Jan-David Nicolas cellular imaging, actin

collaborating groups in Göttingen
Sarah Köster, Tobias Moser, Wiebke Moebius,
Frauke Alves, Reinhard Jahn, Florian Rehfeldt

DESY:
Michael Sprung, Alexey Zozulya, Eric Stellamanns,

funding:
SFB 755 Nanoscale Photonic Imaging
EXC-172 Molecular physiology of the brain
SFB 937 Collective Behavior of Soft and Biological Matter
SFB 803 Functionality by organisation of membranes…

Motivation: Quantitative Synaptology (SFB 1286, Göttingen)

understand structure and function of one synapse quantitatively –> virtual synapse

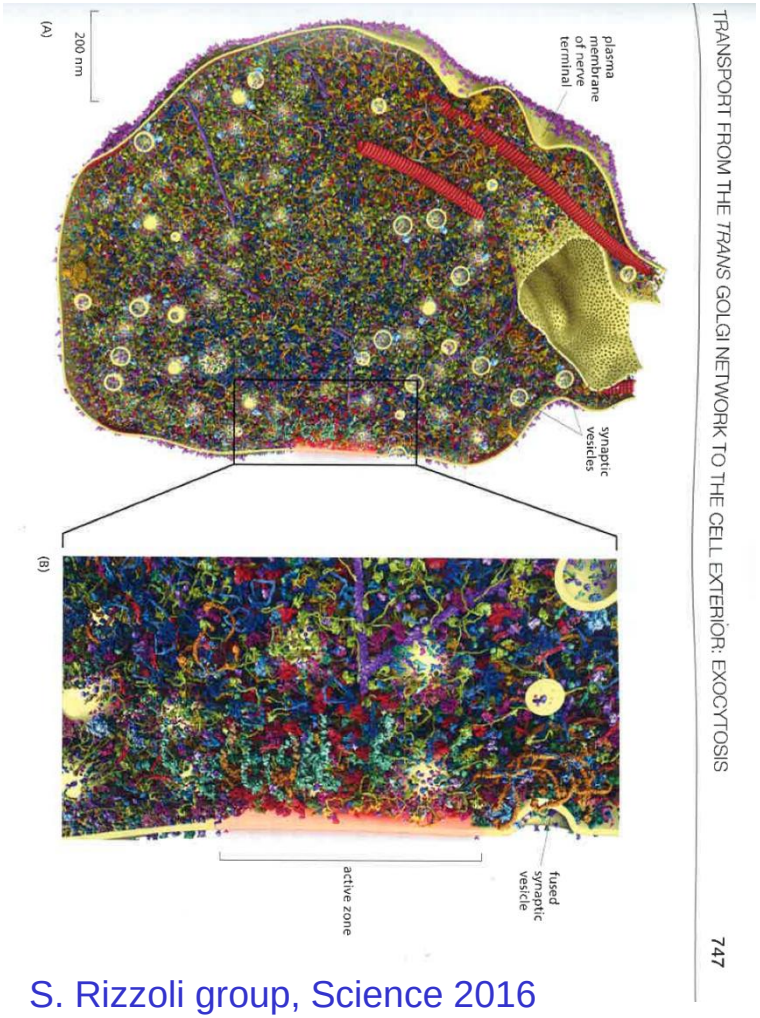

S. Rizzoli group, Science 2016

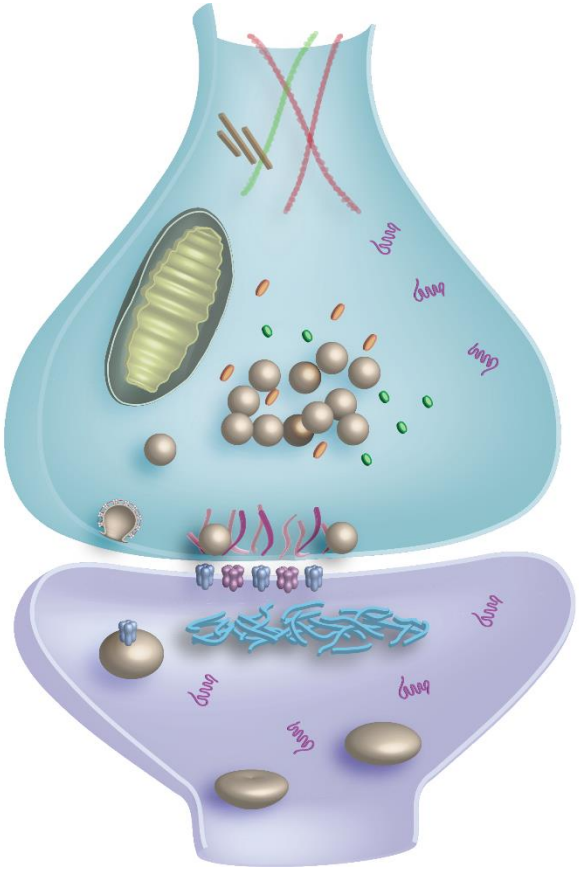

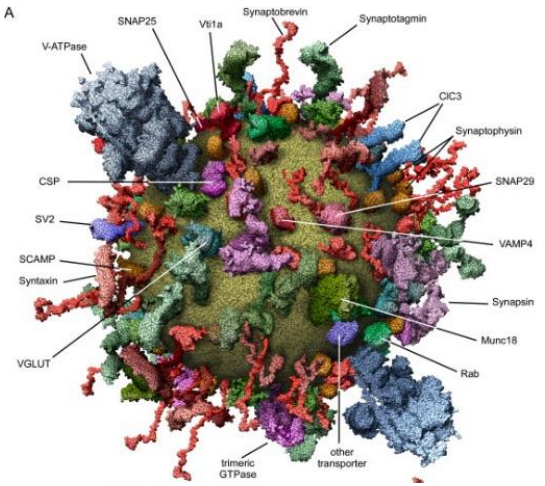

SAXS of synaptic vesicles
S. Castorph et al., Biophys.J 2009
collaboration: R. Jahn

Motivation: The connectivity of the brain

.. human brain has 10^{11} neurons and 10^{14} synapses

connectivity determines function

require sufficient field of view and resolution

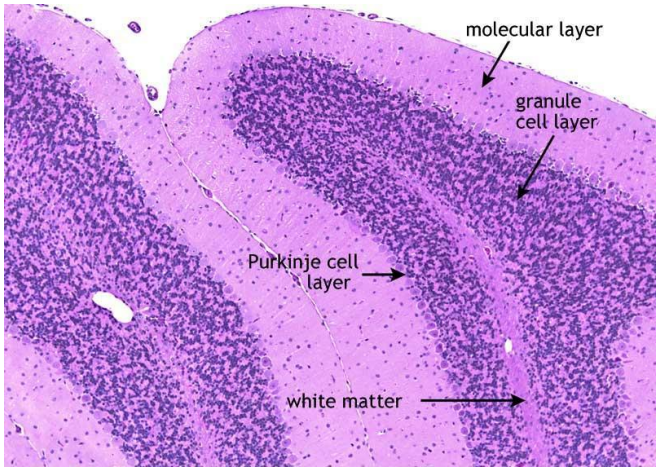

http://www.histology-world.com/photoalbum/displayimage.php?album=97&pid=1099

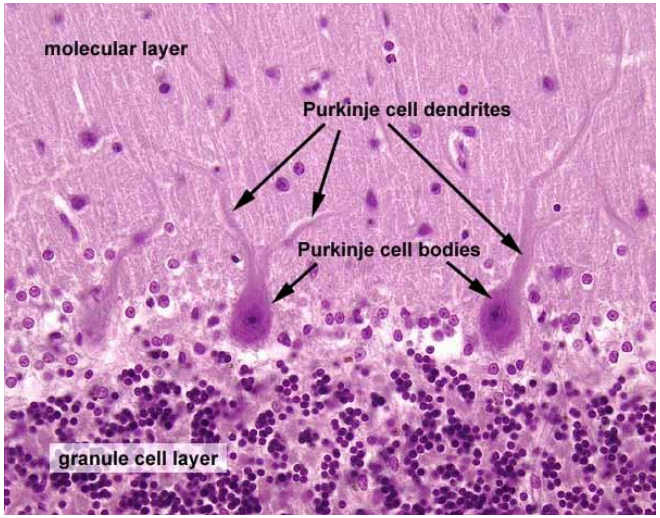

http://www.siumed.edu/~dking2/ssb/NM031b.htm

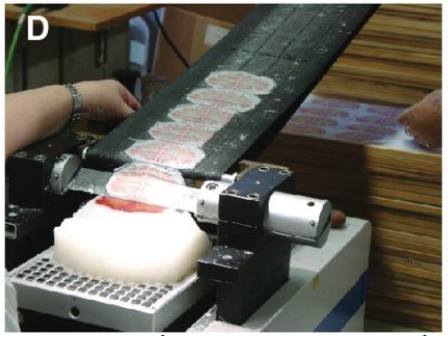

- Amunts et. al. , Science (2013)
  - sentire human brain
  - 7404 histological sections
  - width 20 µm

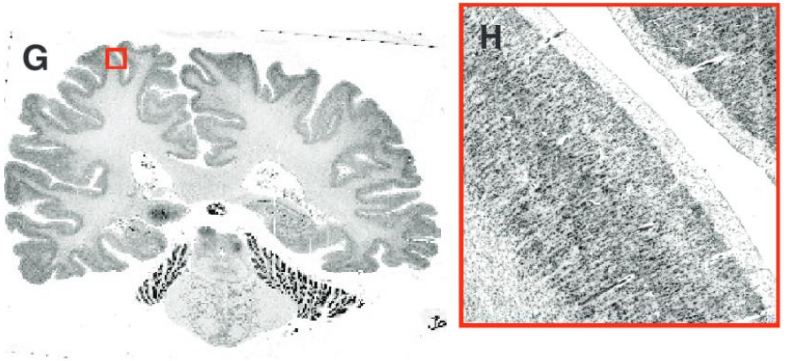

- gold standard: histology

  fixation, dehydration, clearing, impregnation, embedding,sectioning, slide staining

bridge the length scales

structural biophysics

- **biomolecular assembly**
- **in-vitro to cell to tissue**
- **3D spatial arrangement**

X-ray

- **field-of view / 3D**
- **Quantitative contrast**
- **resolution**

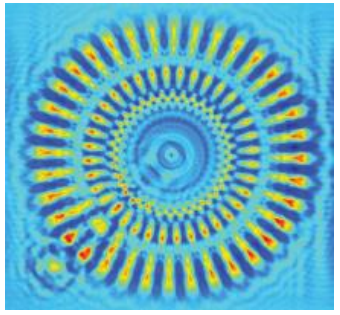

(nano)-diffraction

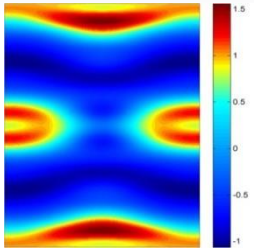

biomolecular assemblies

res / FOV

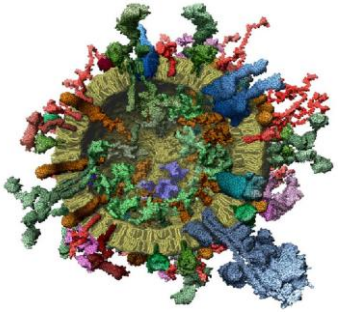

0.5 nm
50 nm

ptychography

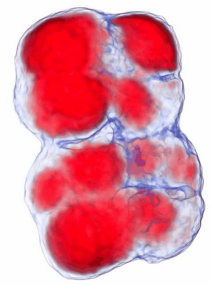

cells

50nm
5µm

propagation imaging

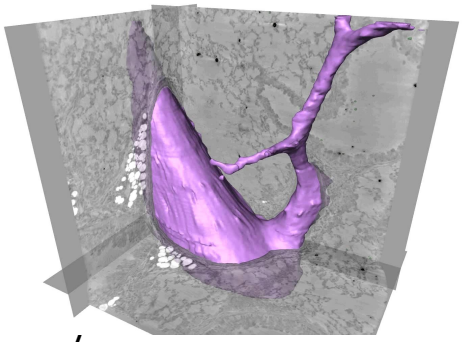

tissue / organs

0.5µm
500µm

µ-focus CT (lab)
grating

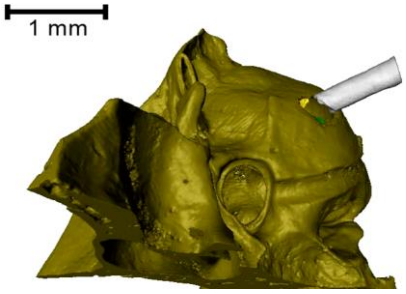

5µm
5mm

I.
high resolution holography and tomography

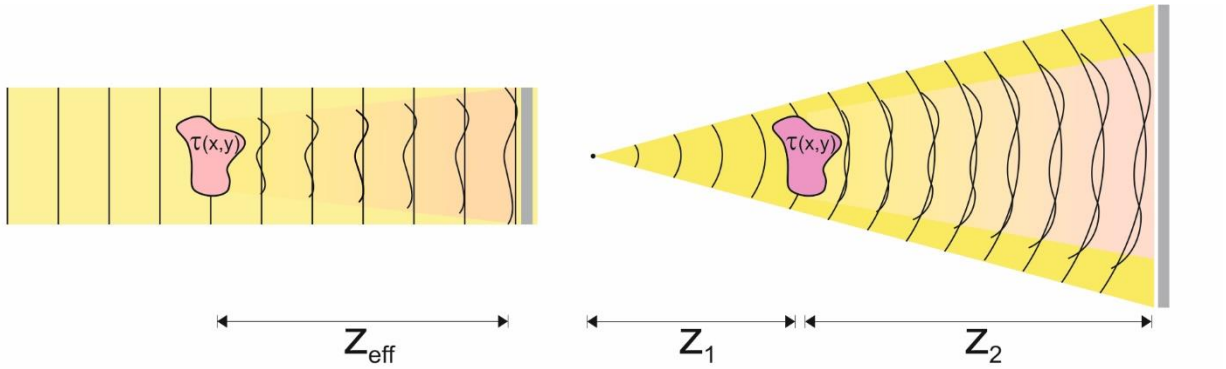

$$z_{eff} = \frac{z_1 z_2}{z_1 + z_2}$$

$$M = \frac{z_1 + z_2}{z_1}$$

II.
human neuroanatomy

III.
dynamical tomography

Imaging formation: Fresnel diffraction integrals

$$\psi(x',y',z) = \frac{1}{i\lambda}\int_{-\infty}^{\infty}\int_{-\infty}^{\infty}\psi(x,y,0)\frac{1}{r}\exp(ikr)\frac{1+\cos(\vec{n}\cdot\vec{r})}{2}dxdy \qquad \psi(x,y,0) = \psi_0\,\tau(x,y)$$

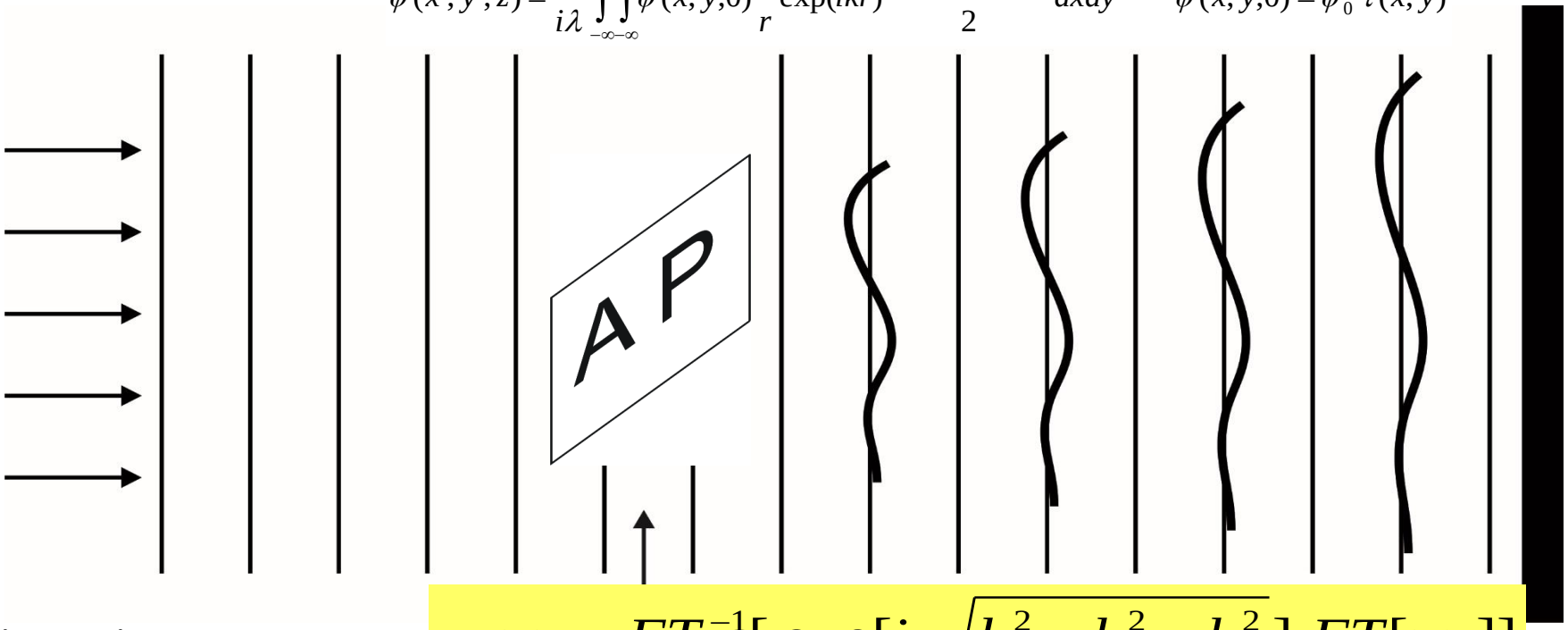

object with complex transmission function τ(x,y)

$$\psi_z = FT^{-1}[\,\exp[iz\sqrt{k^2 - k_x^2 - k_y^2}\,]\;FT[\psi_0]]$$

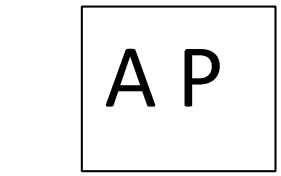

Absorption Phase

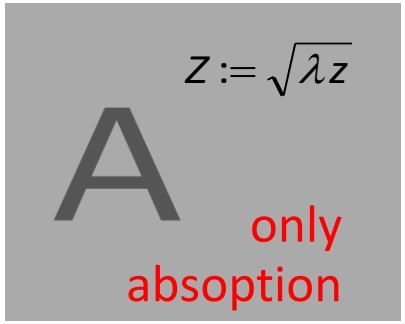

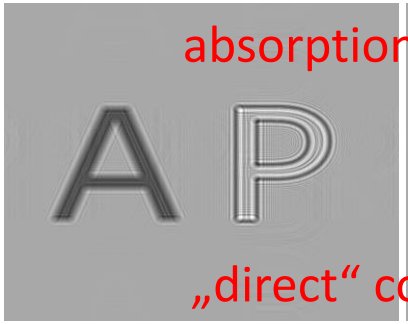

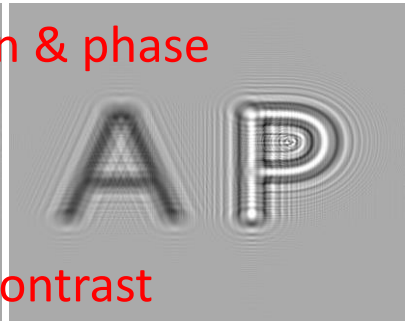

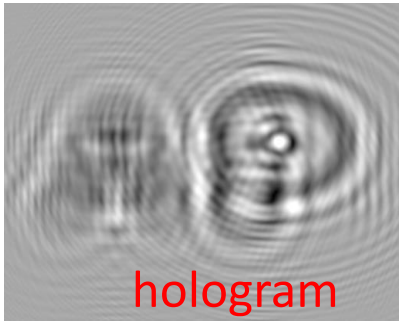

Propagation imaging with x-rays pioneered by S.Wilkins et al. 1996, P. Cloetens et al. et al. 1999;

Image formation

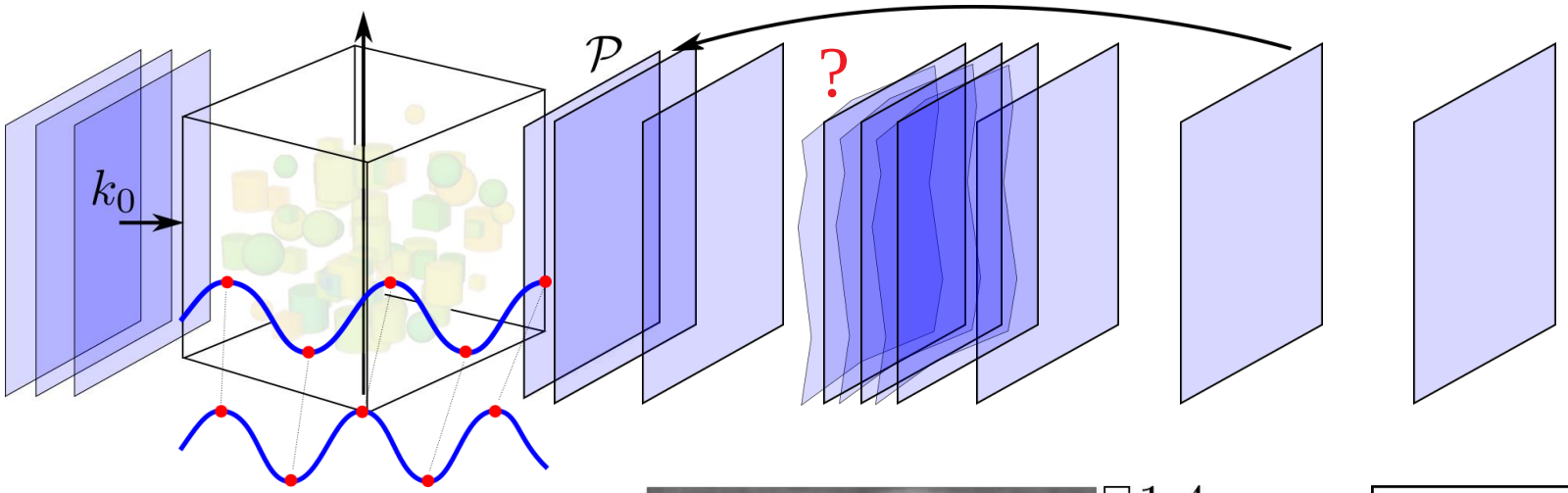

Dennis Gabor

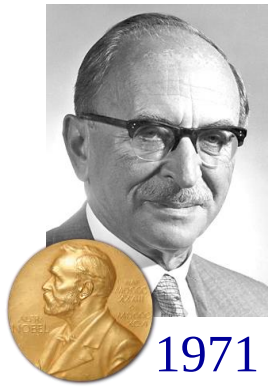

1971

$$n = 1 - \delta + i\beta$$

$$\mathrm{H_{50}C_{30}N_9O_{10}S_1}$$

$$\varrho \approx 1.35\,\mathrm{g/cm}$$

@ 10 keV: $\beta \approx 7 \cdot 10^{-9}$, $\delta \approx 3 \cdot 10^{-6}$

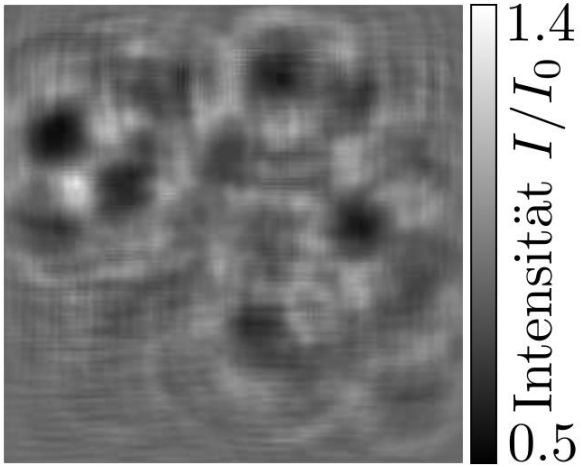

?

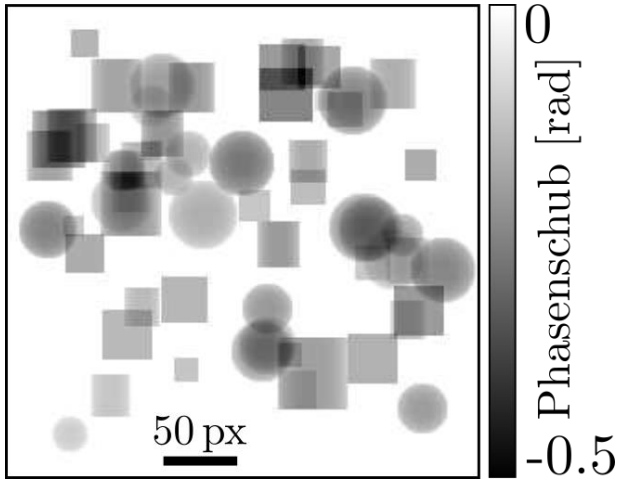

example by A.. Ruhlandt

Image reconstruction

$$\nabla_{xy} \cdot [I(x,y,z)\ \nabla_{xy}\phi(x,y,z)] = -k\frac{\partial I(x,y,z)}{\partial z}$$

transport of intensity eq. (TIE)

$$\partial_z I \approx \frac{1}{\Delta z}\left(I(x,y,z+\Delta z) - I(x,y,z)\right), \quad I(x,y,z) = I_0 = const.$$

Paganin, Gureyev, Mayo, Wilkins
Nugent, Allen& Oxley, Cloetens

$$\nabla^2_{xy}\ \phi(x,y,z)] = -\frac{k}{\Delta z}\left(\frac{I(x,y,z+\Delta z) - I_0}{I_0}\right) \qquad \nabla^{-1}_{xy} = \frac{-1}{q_x^2 + q_y^2 + \alpha}$$

$$\phi(x,y,z)] = \frac{\delta/\beta}{2}\ \ln\left(\frac{4\pi\,\beta}{\delta\lambda\, z} FT^{-1}\left[\frac{FT[I(x,y,z)/I_0]}{q^2 + 4\pi\,\beta/(\delta\lambda\, z)}\right]\right)$$

D. Paganin 2002 (single distance)

$$\phi(x,y,z)] = FT^{-1}\left[\frac{\sum_m FT[I(x,y,z_m)]\sin(4\pi\, q^2/\lambda\, z)}{\sum_m 2\sin(4\pi\, q^2/\lambda\, z) \ + \ \alpha}\right]$$

P. Cloetens 1999 (m distances, holotomography, CTF-basedI

one way or another all based on linearisation !

Image reconstruction

holographic reconstruction

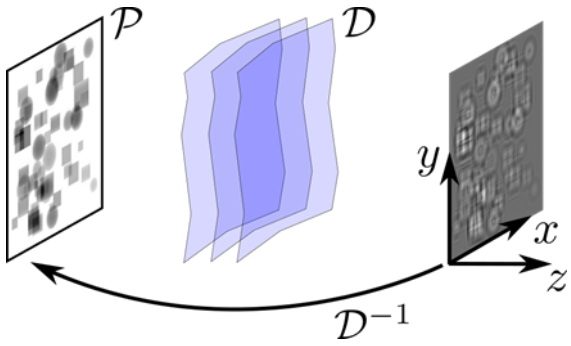

contrast transfer function

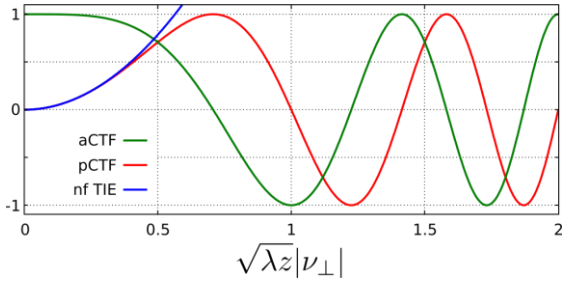

$$\mathcal{F}\left[\frac{I(x,y,z=d)}{|\Psi_0|^2}\right] \approx 2\pi\delta_D - 2k\bar{\delta}\sin(\varphi) - 2k\bar{\beta}\cos(\varphi)$$

iterative reconstruction

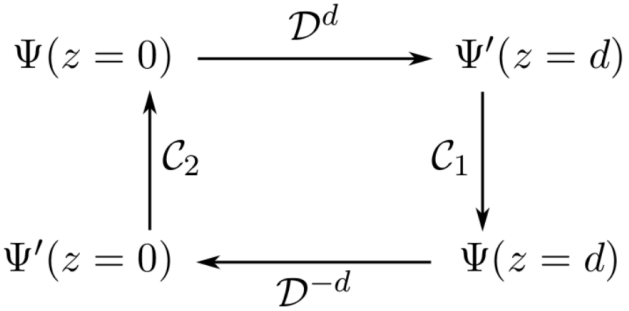

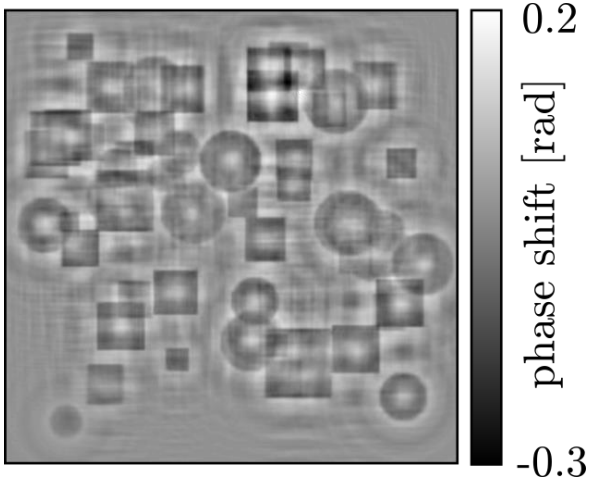

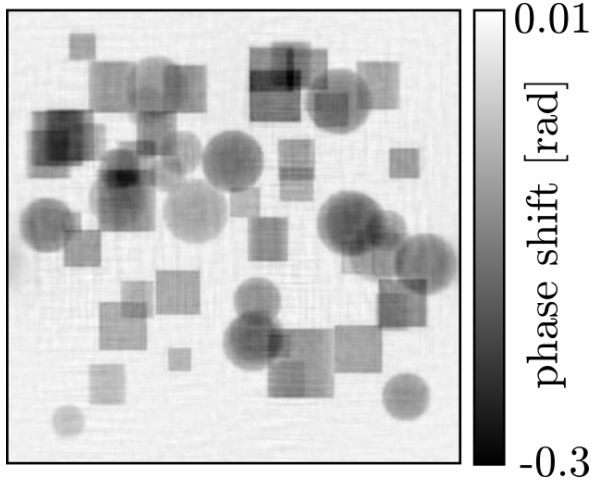

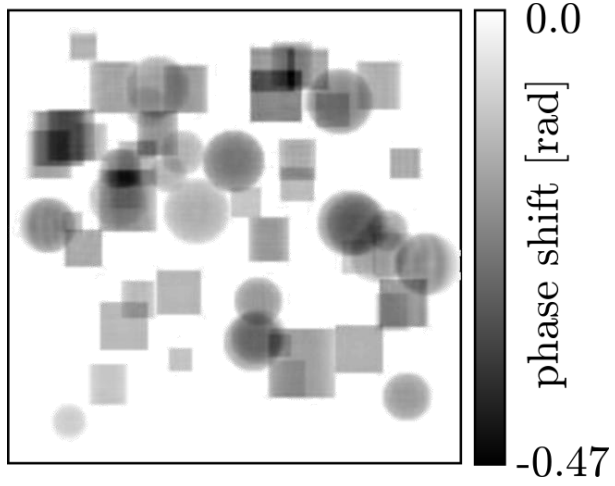

A.. Ruhlandt

Coherent x-ray imaging, phase retrieval and inverse problems

$$I(q_x,q_y) \propto I_0 \left| \int \rho(x,y) e^{i(q_x x + q_y y)} \, dxdy \right|^2$$

iterative projection algorithms
to solve the phase problem

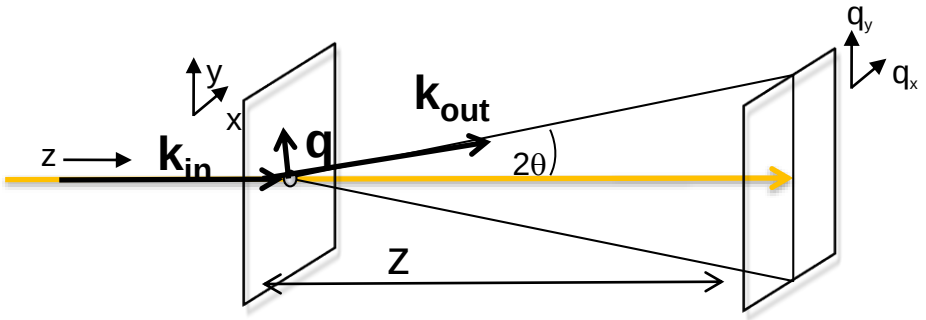

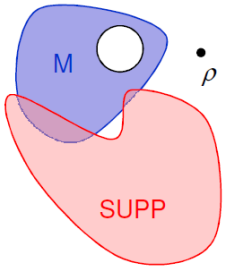

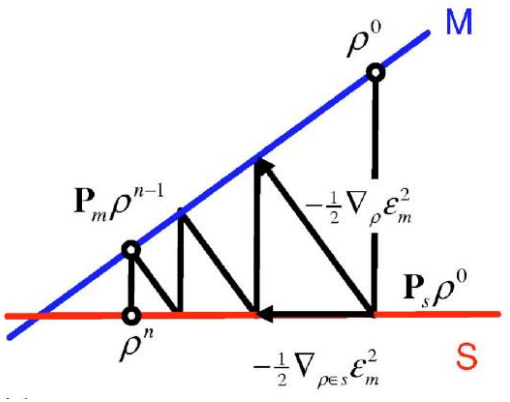

John Miao 1999, Luke 2004, review: J. Miao, M. Murnane, Science 2015

- ***near-field or far-field diffraction***
- ***plane wave versus structured probe (ptychography)***
- ***focused wavefields and designed illumination***
- ***object and wavefront reconstruction***
- ***partial and full coherence***

$$\rho^{n+1} = \left[\frac{1}{2} \beta \left(R_S R_M + I \right) + (1-\beta) P_M \right] \rho^n$$

uniqueness ? convergence ? Poisson data ?
ill-posedness / regularization ?
error metric ? sparsity ? stopping criteria ? missing data ?
resolution per dose / dose fractionation ?

-> single shot reconstruction
-> towards 3D and 4D

adaptation for near-field:

Giewekemeyer et al, PRA 2011; Hagemann et al. , 2015, 2016; Robisch et al., 2015; Krenkel et al., Acta Cryst 2017

Challenges in near-field imaging

$$\nabla^2_{xy}\,\phi(x,y,z)] \;=-\frac{k}{\Delta z}\left(\frac{I(x,y,z+\Delta z)-I_0}{I_0}\right)$$

classical work based on transport of intensity eq. (TIE)

breaks down in the holographic regime !

holo-TIE

M, Krenkel, M. Bartels, T. Salditt, Opt.Express 2013

- ***how to reach high resolution ?***
- ***quantitative reconstruction beyond linearisation ?***
  and with no a prioris, and for a single distance exposure ?
- ***probe abberations (empty beam normalisation)***

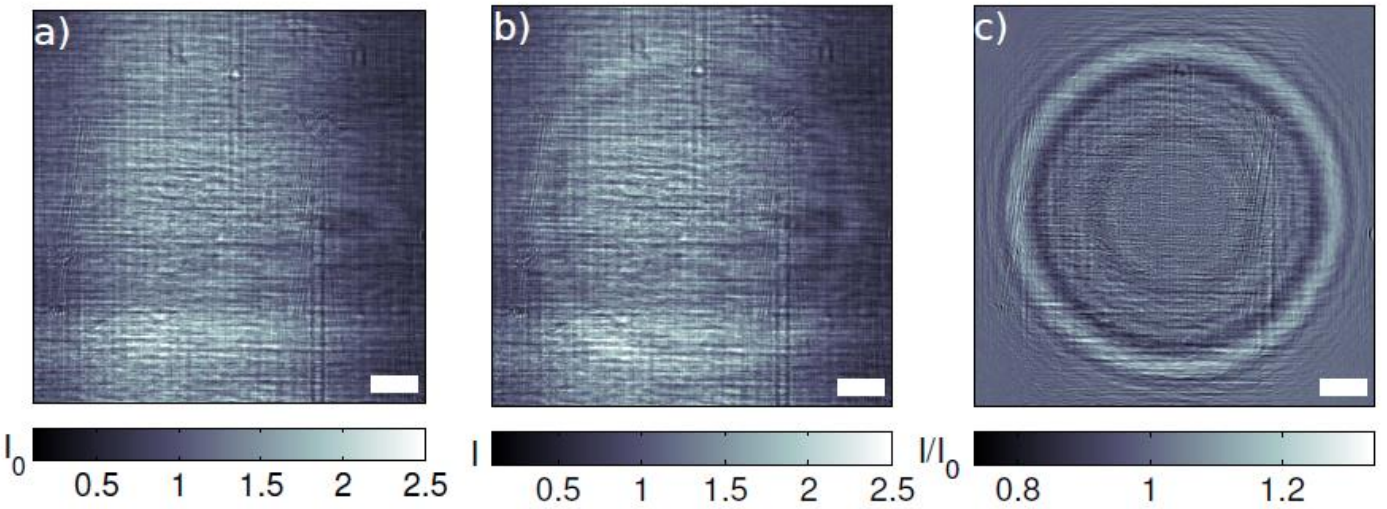

Near-field imaging beyond idealizing assumptions on the probe

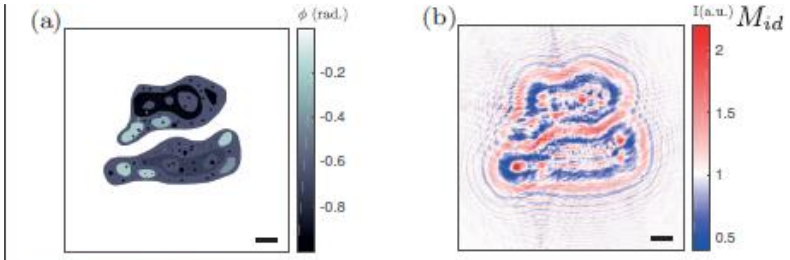

probe is important for resolution & image quality

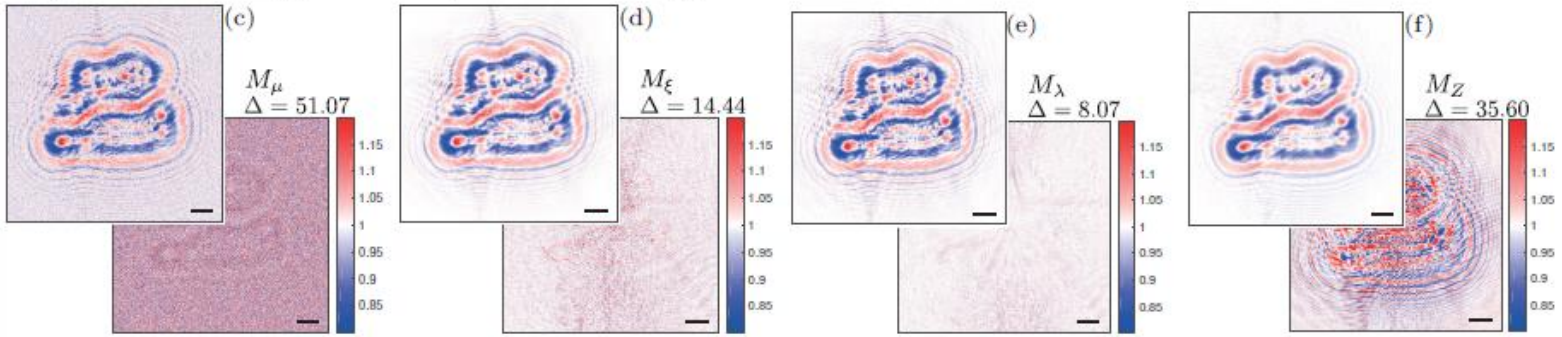

Poisson noise
$\mu = 100$ ph/px

coherence length
$\xi = 100$ px

finite bandwidth
$\Delta\lambda/\lambda = 10^{-2}$

beam distortions
Zernike

- (partially-)coherent: $\xi < \infty$
- non monochromatic: $\Delta\lambda/\lambda > 0$
- finite source size
- probe aberrations

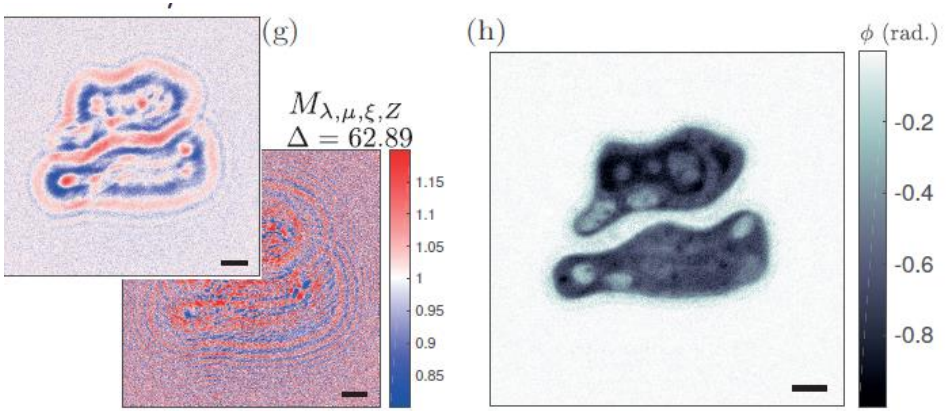

all together

reconstruction

J. Hagemann et al. Opt.Expr. 2014
C. Homann et al. PRA 2014
J. Hagemann, Diss. thesis 2017

Near-field ptychography at ID16 A

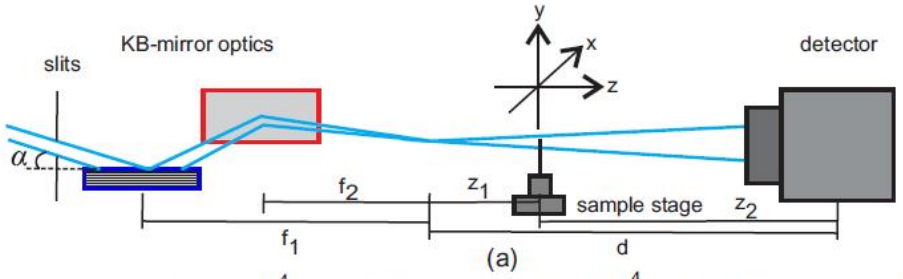

$$p_1^{k+1} = p_1^k + \alpha D_{-\Delta_{1,j}} \left[\frac{\left(P_M \left[\psi_j^{(i)k} \right] - \psi_j^{(i)k} \right) [o^{(i)k}]^*}{\left| o^{(i)k} \right|^2} \right]$$

$$o^{(i)k+1} = \left[o^{(i)k} \right] + \beta \frac{\left(P_M \left[\psi_j^{(i)k} \right] - \psi_j^{(i)k} \right) D_{\Delta_{1,j}} \left[p_1^{k+1} \right]^*}{\left| D_{\Delta_{1,j}} \left[p_1^{k+1} \right] \right|^2},$$

Simultaneous probe and object reconstruction for the near-field
A. Robisch, K. Kröger, A. Rack, TS, N.J.Phys. 2015

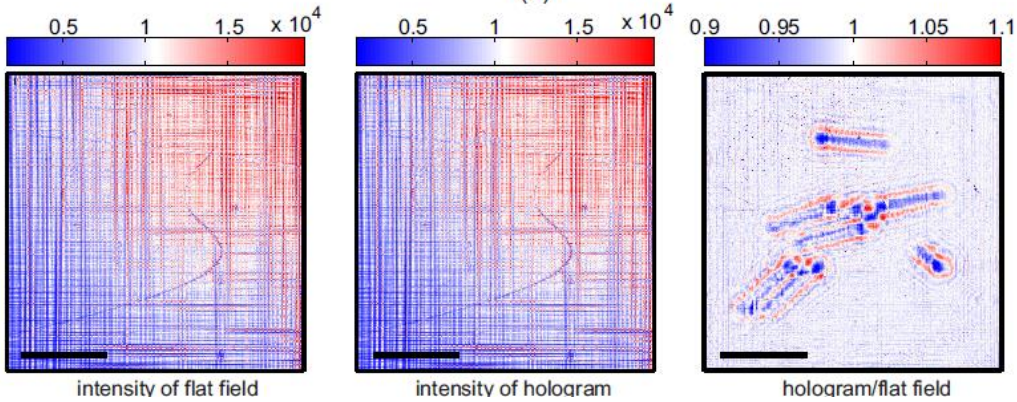

nanowires, 17.5 keV, 26x39nm focus
4 defocus planes, 16 lateral positions

flat field correction is flawed !

meet your probe!

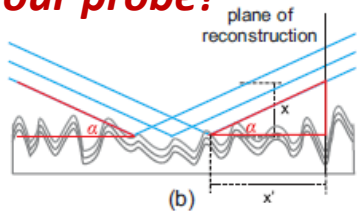

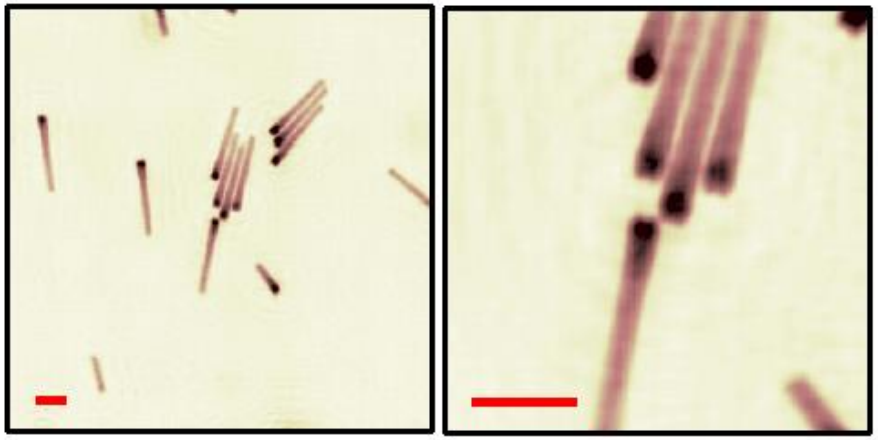

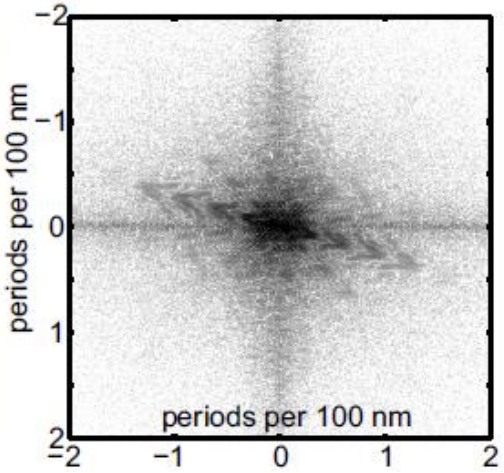

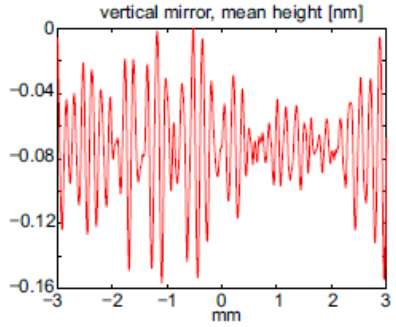

A.-L. Robisch et al., Opt.Lett. 2016

Reconstructed object: nano wires with sub 100 nm resolution

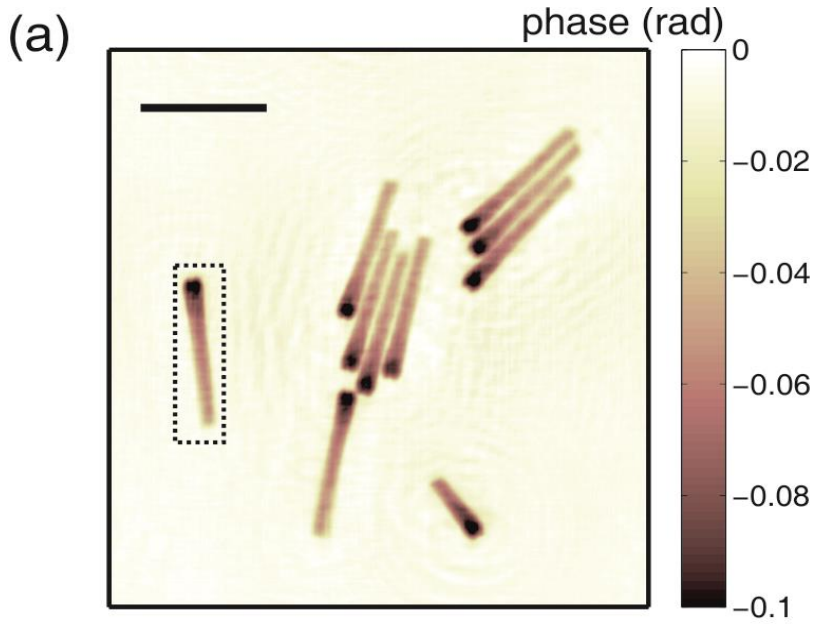

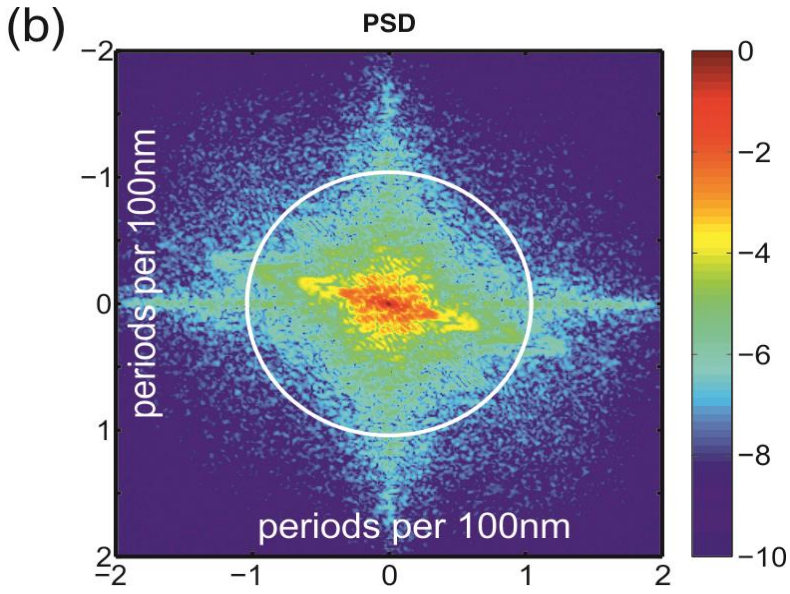

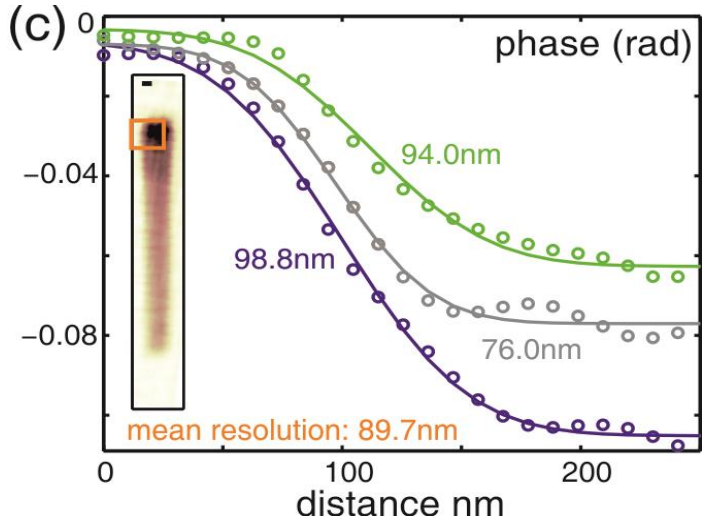

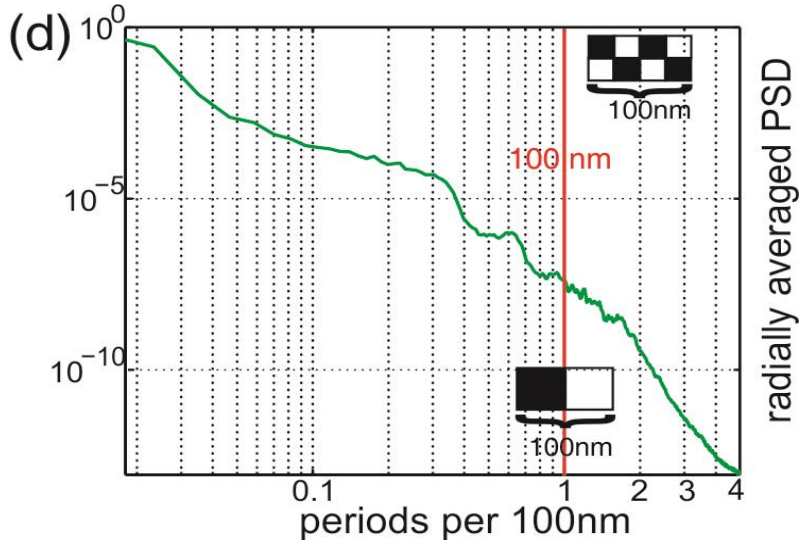

A.-L. Robisch et al., Opt.Lett. 2016

Near-field probe reconstruction

nano-focus KB GINIX@P10/ PETRAIII
multiple magnitude projection (mmMMP)
RAAR-like scheme, no or loose support

detection plane

near-focal plane

variation of NA by KB slits

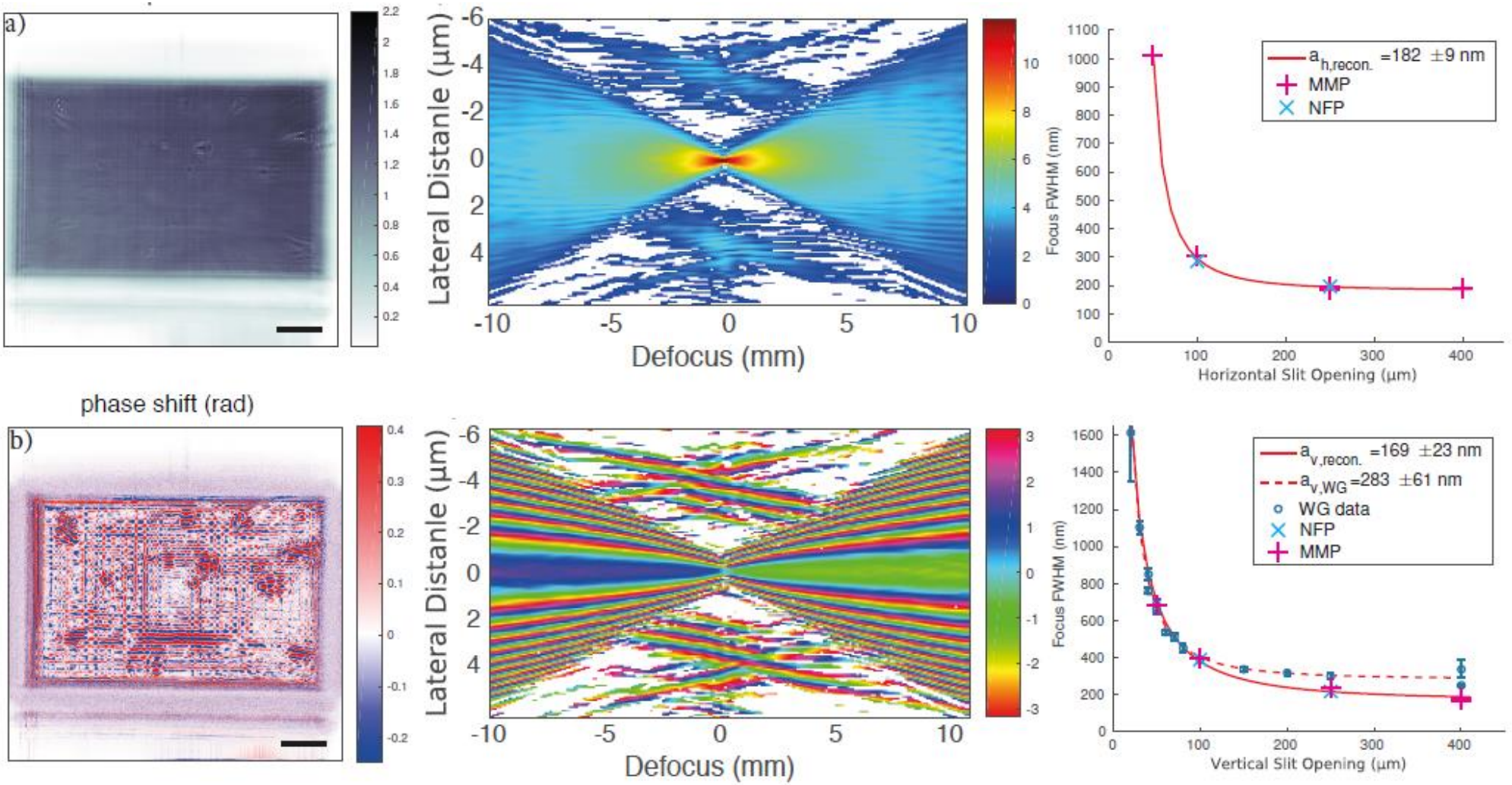

J. Hagemann, A.-L- Robsich, M. Osterhoff, T. Salditt J.Synchr.Rad. 2017

but: assuming full coherence

Reconstruction mode mixture in the near-field

near-field analogue to Thibault & Menzel , Nature (2013)
numerical simulation of partially coherent probe (3modes)
QR factorisation (unitary modes); occupation number λ_m
multi-mode multiple magnitude projection (mmMMP)
RAAR-like scheme

$$I_m = |\mathcal{D}_{\mathrm{Fr}}(\Psi_m)|^2 \qquad \mathcal{I} = \sum_m \lambda_m I_m$$

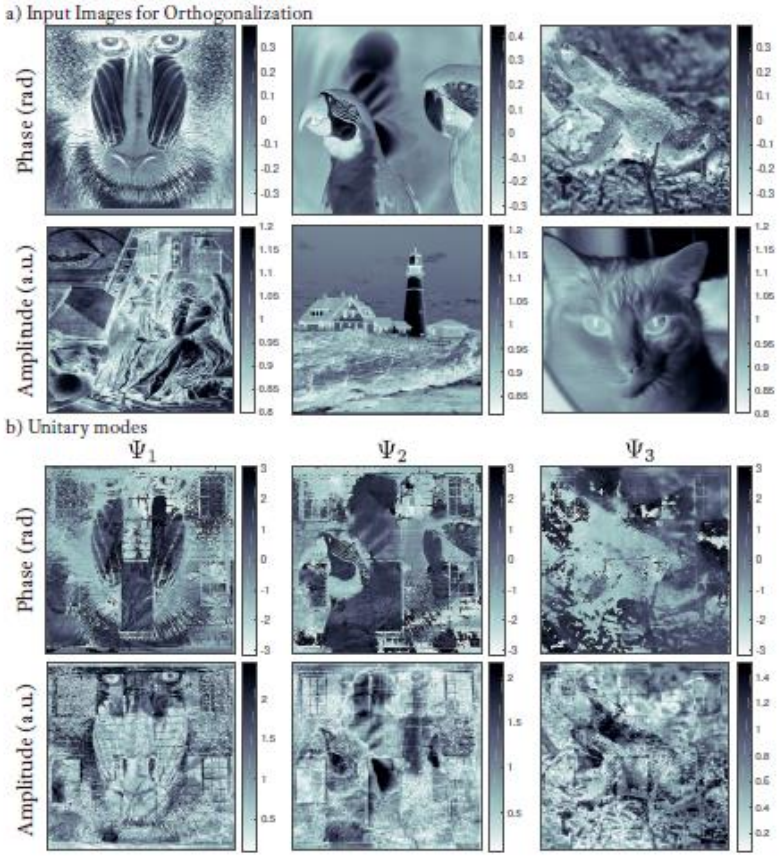

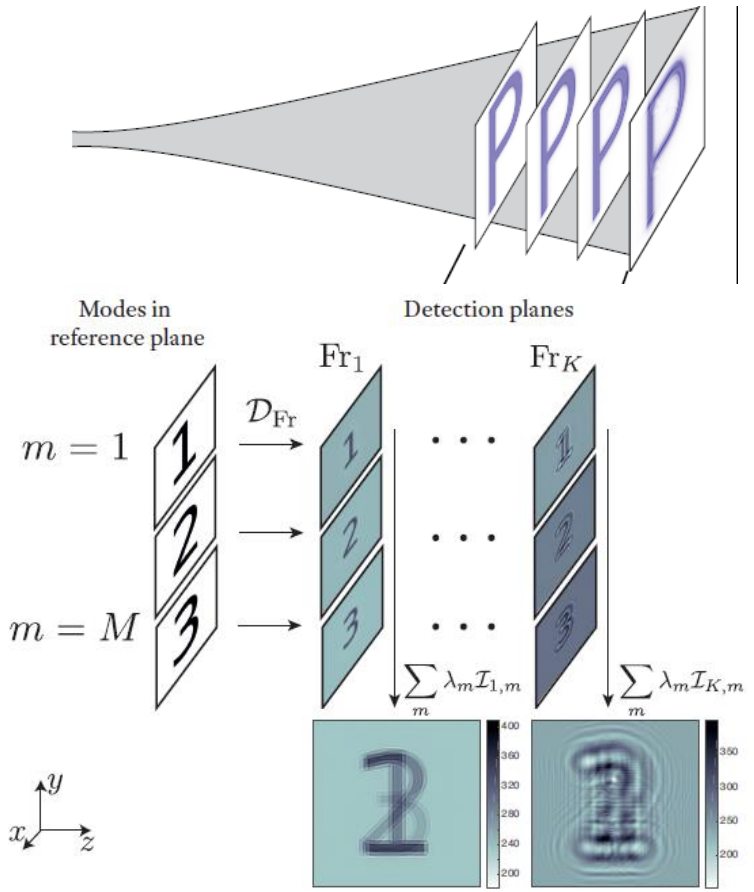

adaptation to measurement

$$A_{\mathcal{I}_k}(\bullet) = \sqrt{\frac{I_{k,m}}{\sum_{m=1}^{M} I_{k,m}}} \cdot \sqrt{\mathcal{I}_k} \cdot \exp(i \arg(\bullet))$$

J. Hagemann, T. Salditt Opt.Express 2017

Comparison of the degree of coherence

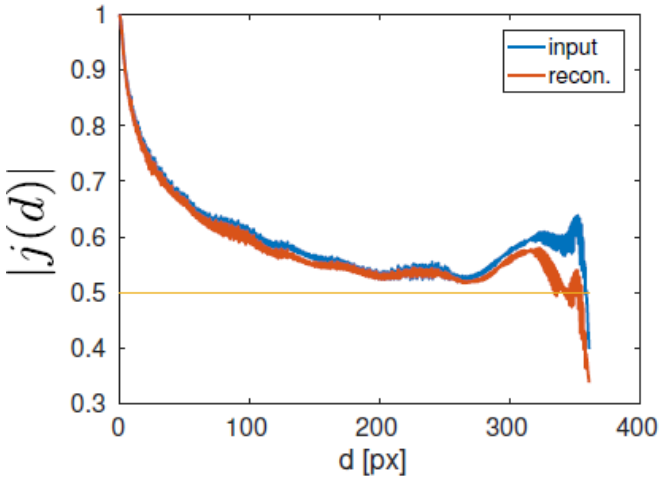

$$J_m(\vec{r_1}, \vec{r_2}) = \Psi_m(\vec{r_1})\Psi_m(\vec{r_2})^*$$

$$J(\vec{r_1}, \vec{r_2}) = \sum_m \lambda_m J_m(\vec{r_1}, \vec{r_2})$$

$$j(\vec{r_1}, \vec{r_2}) = \frac{J(\vec{r_1}, \vec{r_2})}{\sqrt{J(\vec{r_1}, \vec{r_1})}\sqrt{J(\vec{r_2}, \vec{r_2})}}$$

Evolution of the occupation numbers

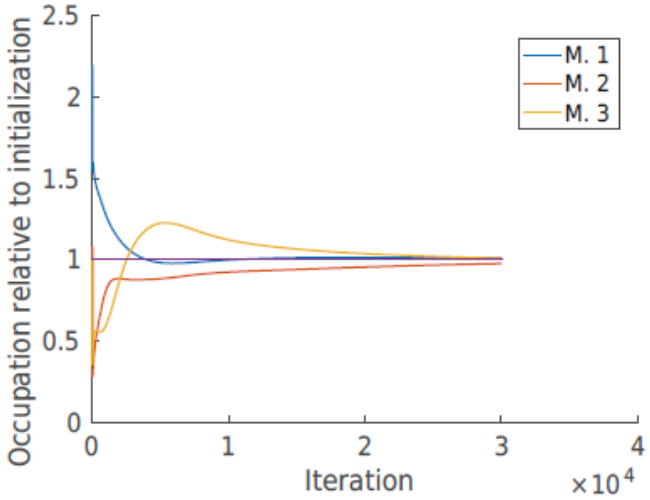

Error per pixel for all measurement planes -
How many modes are needed for the reconstruction?

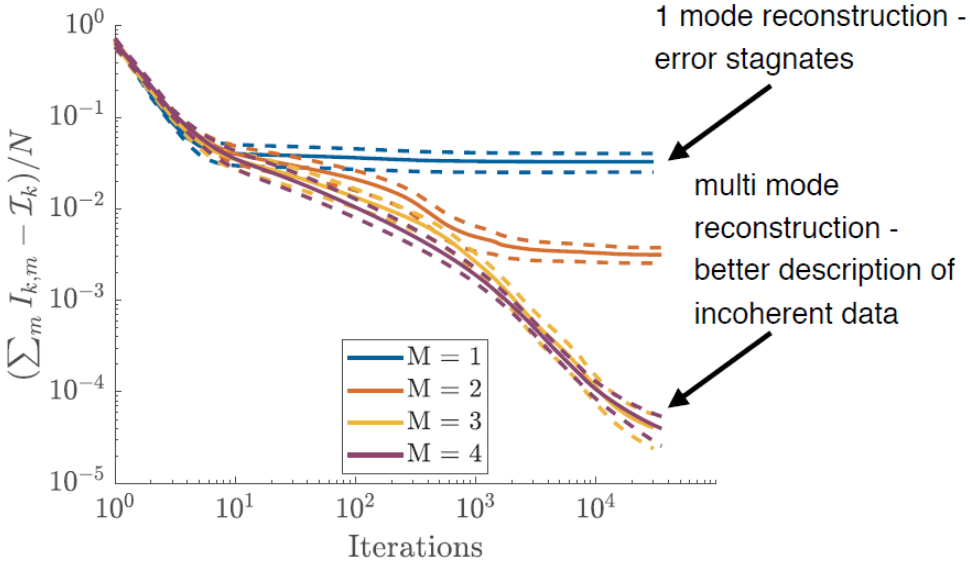

J. Hagemann, T. Salditt Opt.Express 2017

Coherence-Resolution relationship

influence of lateral coherence length ξ on reconstruction quality

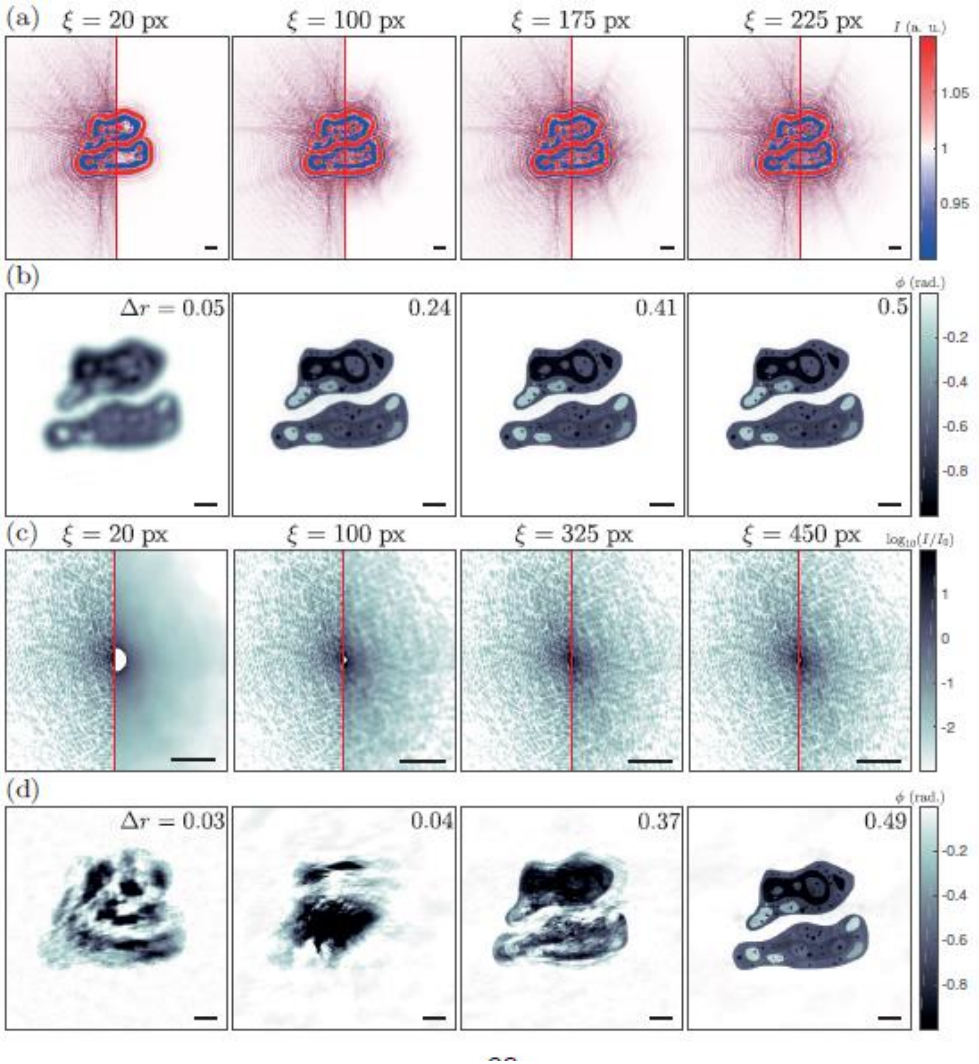

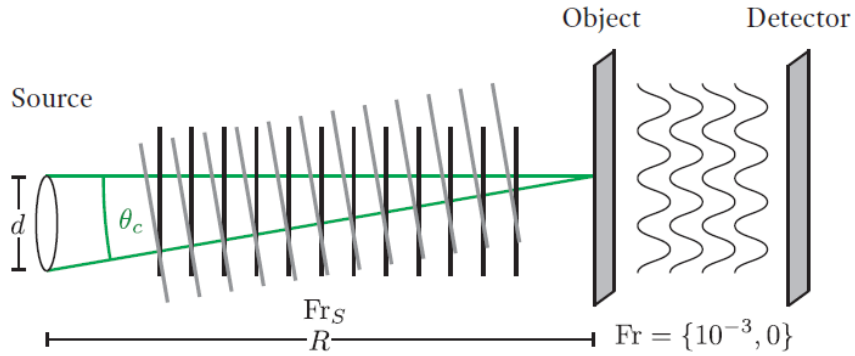

$$\xi = \frac{\lambda}{2}\frac{R}{d} = \frac{\lambda}{2}\frac{1}{\theta_c}, \qquad \theta_c = \frac{\lambda}{2\xi}$$

natural units:

ξ in pixel, Fresnel number F

$$q(\alpha) = \frac{2\pi}{\lambda}\sin(\alpha) \qquad \alpha \in \{-\theta_c/2, \theta_c/2\}$$

$$\alpha = \zeta\theta_c/2,\ \zeta \in \{-1, 1\}, \qquad q = \frac{\pi\zeta}{2\xi}$$

- *simulate partial coherence*
- *equivalent to convolution of hologram*
- *but in reconstruction:*
  falsely assume full coherence & compute error

J. Hagemann, T. Salditt Opt.Express 2017b

Coherence-Resolution relationship

example: coherence length ξ = 200 px

NFH (near-field holography) versus CDI

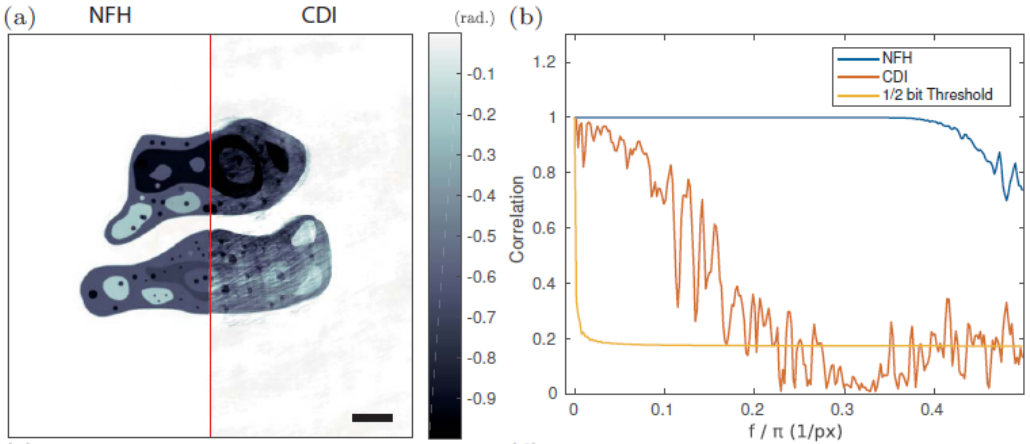

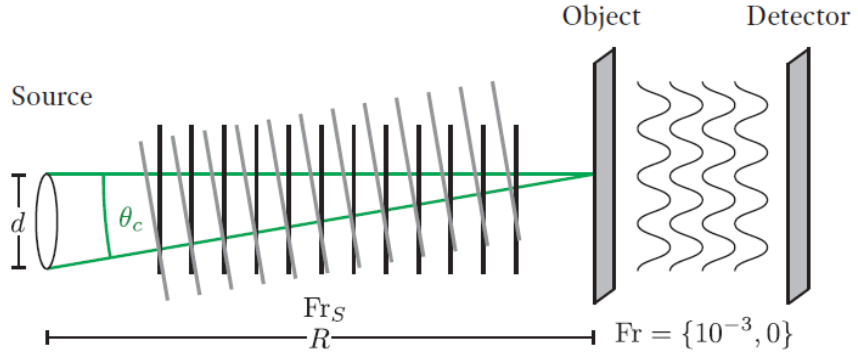

$$\xi = \frac{\lambda}{2}\frac{R}{d} = \frac{\lambda}{2}\frac{1}{\theta_c}, \qquad \theta_c = \frac{\lambda}{2\xi}$$

natural units:

ξ in pixel, Fresnel number F

$$q(\alpha) = \frac{2\pi}{\lambda}\sin(\alpha) \qquad \alpha \in \{-\theta_c/2, \theta_c/2\}$$

$$\alpha = \zeta\theta_c/2, \zeta \in \{-1, 1\}, \qquad q = \frac{\pi\zeta}{2\xi}$$

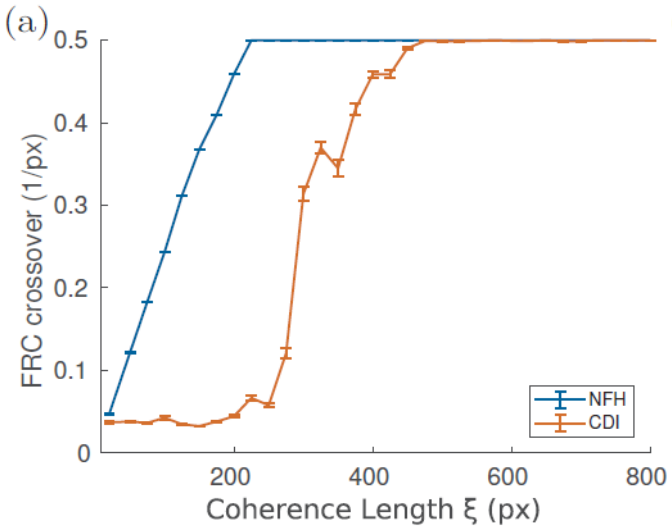

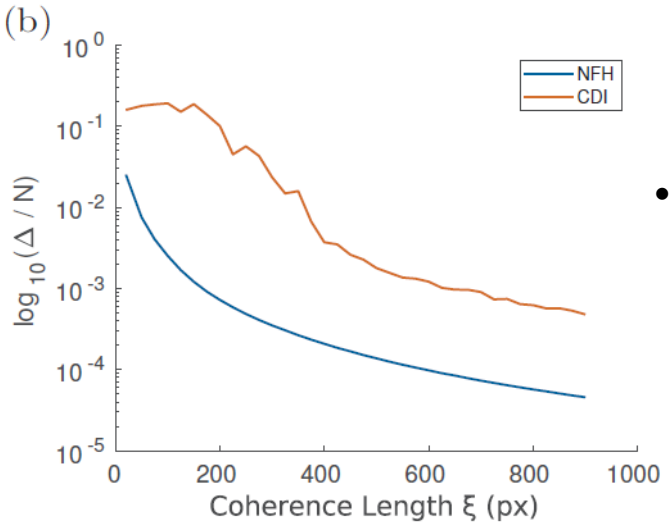

- *NFH more tolerant than CDI towards partial coherence*

but so far: many measurements
how about single FEL pulse ?

J. Hagemann, T. Salditt Opt.Express 2017b

Simultaneous probe and object reconstruction from single shot

2 detection planes: empty beam and object in beam recorded simultaneously

transparent scintillator and mirror in front of object

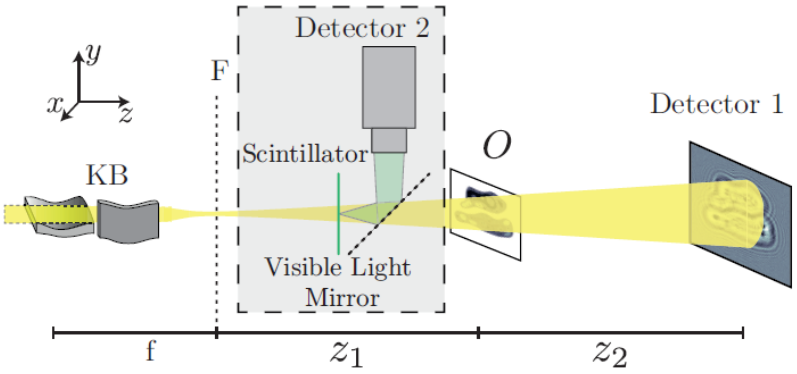

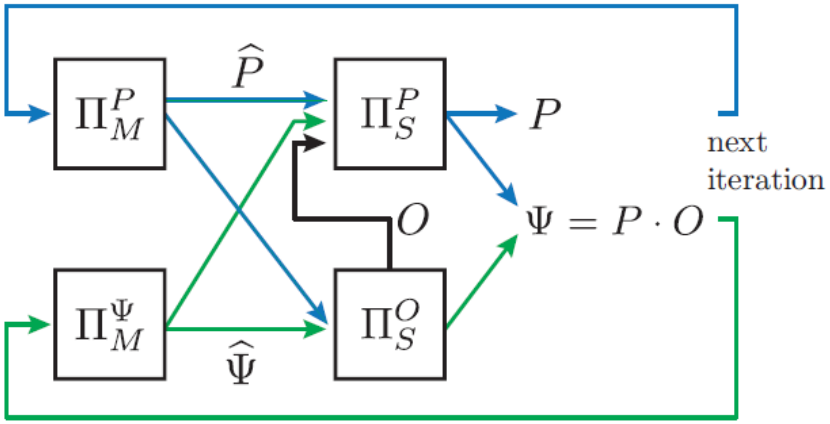

devide & update algorithm

2 measurements and seperability

conv. empty beam division

devide& update

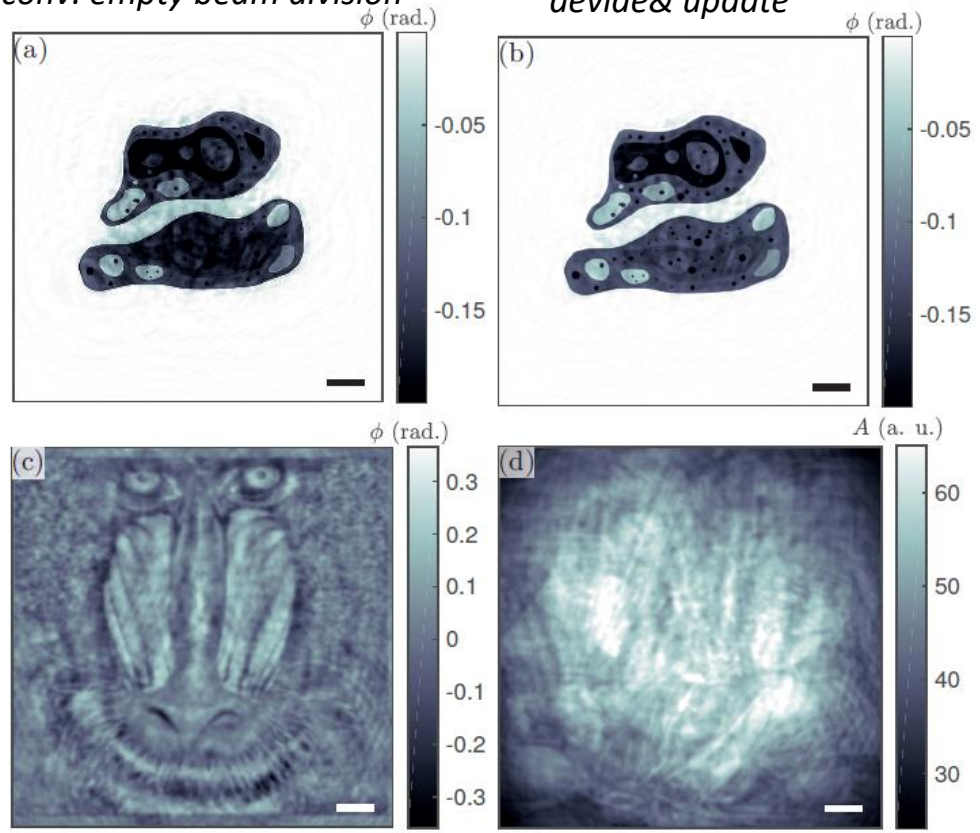

Fig. 6. Results obtained with divide&update for simulated noisy data with μ = 200 ph/px after 4000 iterations. (a) The reconstructed object phases, obtained from conventional flat-field corrected data using RAAR. (b) The reconstructed object obtained from d&u. (c) Phases and (d) amplitudes of the reconstructed probe. The scale bar indicates 50 px.

J. Hagemann, T. Salditt, Opt. Expr. 2017b

Waveguide holographic imaging

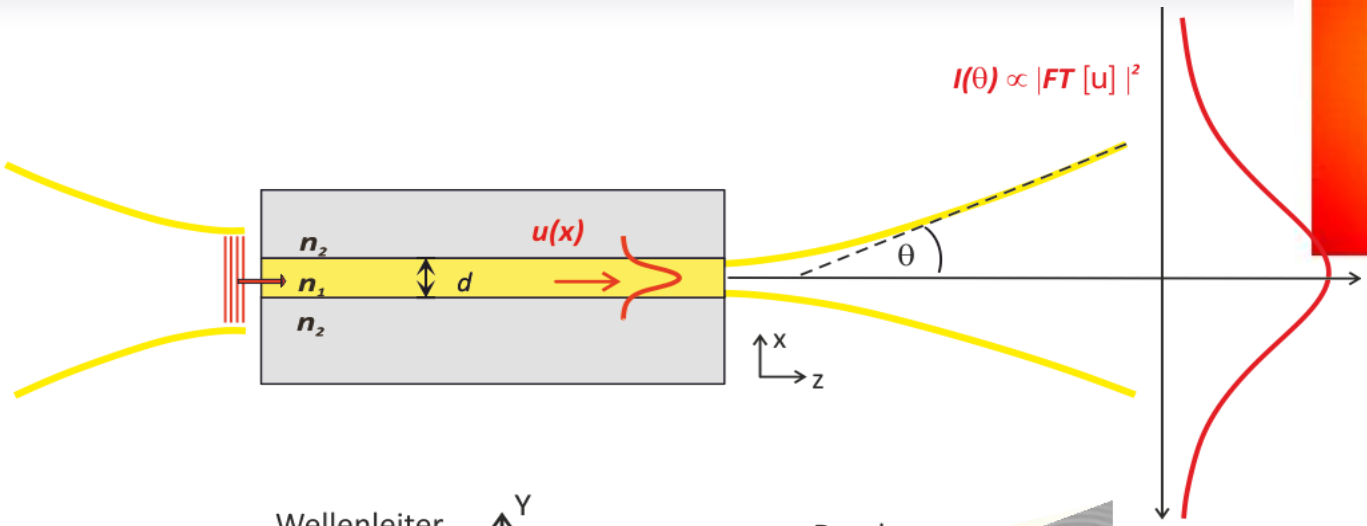

20 nm x 17 nm, I_0=2x10^9 ph/s 8 keV

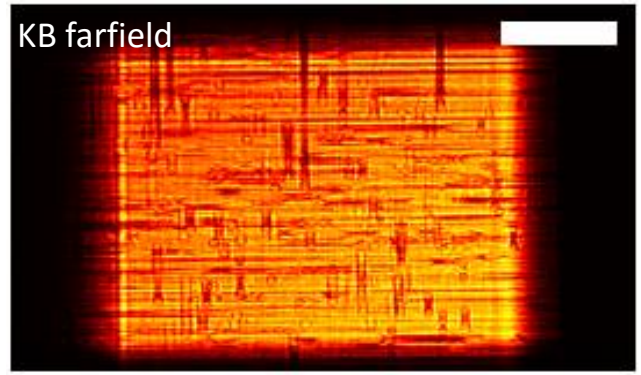

200 nm x 200 nm I_0>10^{11} ph/s

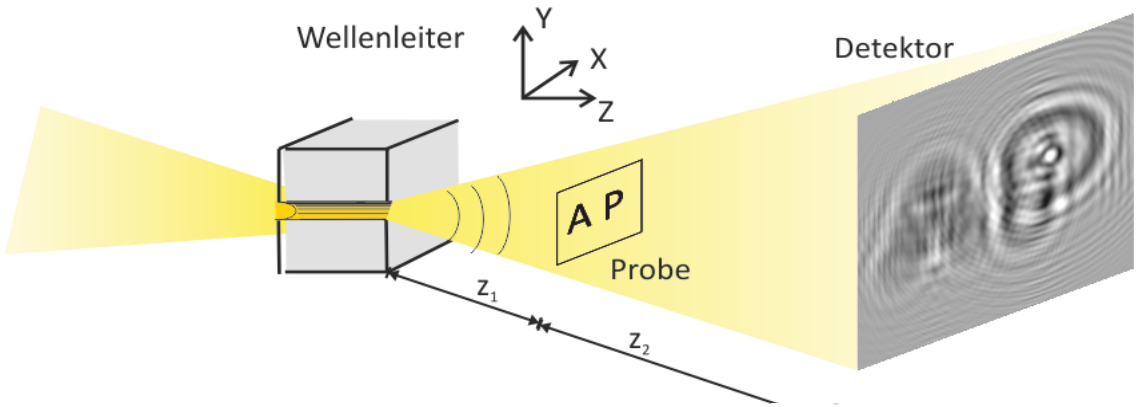

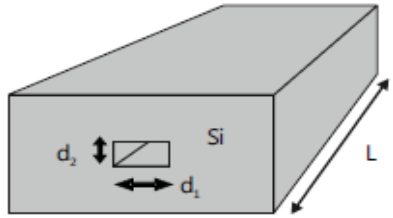

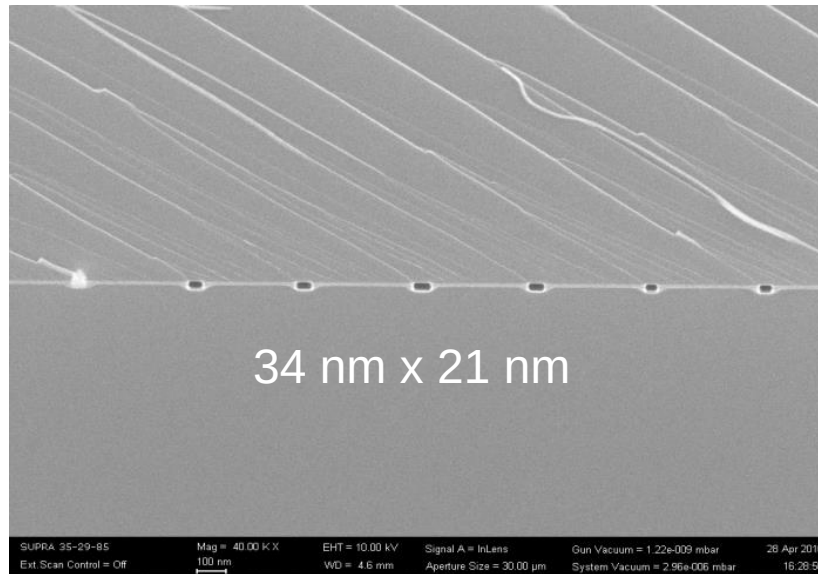

A. Jarre et at., Phys.Rev.Lett. 2005, C. Fuhse et al, Phys.Rev.Lett. 2006
T. Salditt et al., Phys. Rev. Lett. 2008
S. Krüger et al., Opt. Express 2010; Krüger et al. J. Synchr. Rad. 2012,
M. Osterhoff, T.Salditt NJP, 2012, H. Neubauer, et al., JAP 2014

GINIX – the Göttingen Instrument for Imaging with X-rays at beamline P10/PETRAIII

Photo: M. Osterhoff

KB nano-focus: 200 nm spot size, 10^{11} ph/sec, 5-15 keV
waveguide optics, ptychography, nano-diffraction, holography
upgrade: time resolved imaging

Kalbfleisch et al. AIP Conf. 2011, Salditt et al JSR 2016

Coherence propagation, coupling, and model filtering

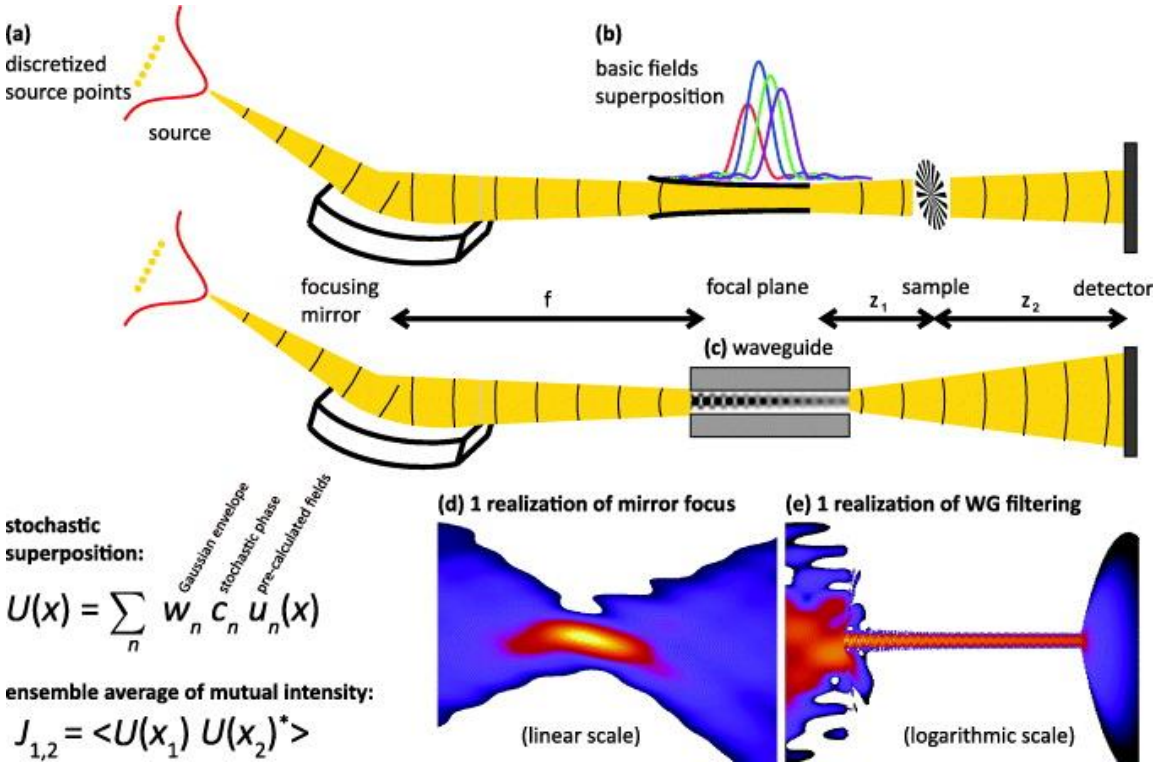

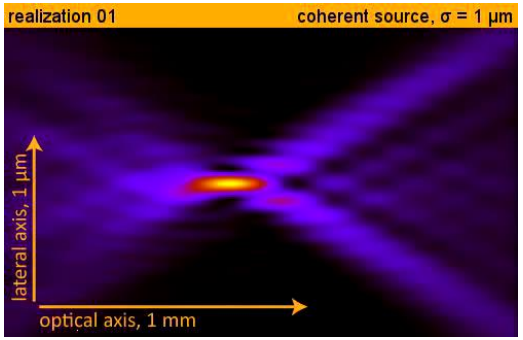

different stochastic realisations of the field

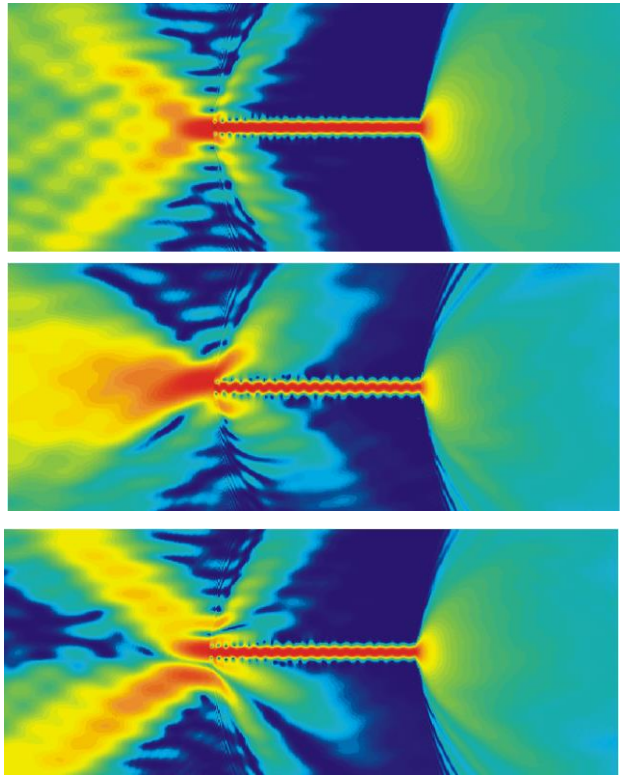

- *decouples coherence from the source*
- *„slits“ down the beam*
- *quasi-spherical source,*
- *nearly aberration free, dispersion free*
- *after optimization: about 1e9 ph/sec (GINIX, P10)*

M. Osterhoff ,T. Salditt, NJP 2011

holographic imaging example

Test pattern in 200 nm Gold, 13.8 keV

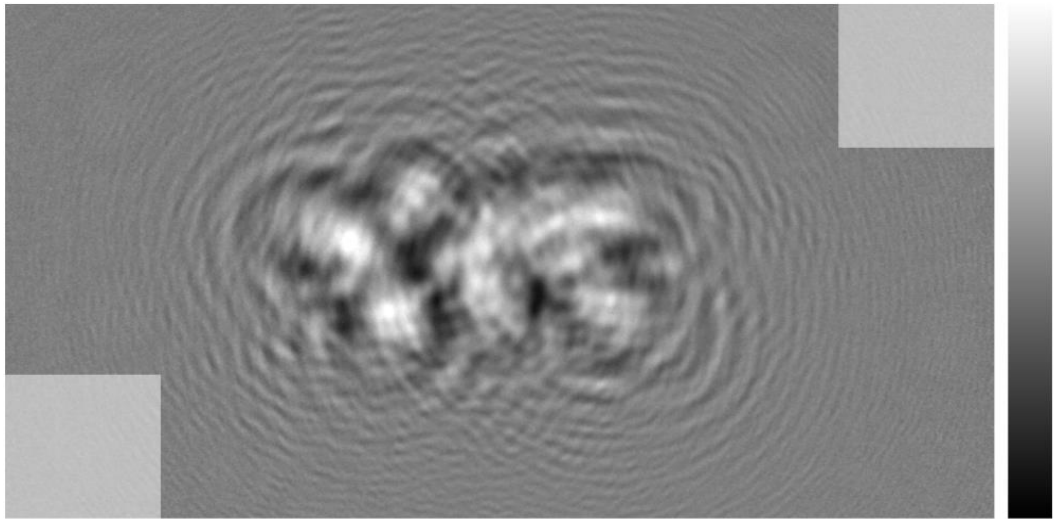

mHIO

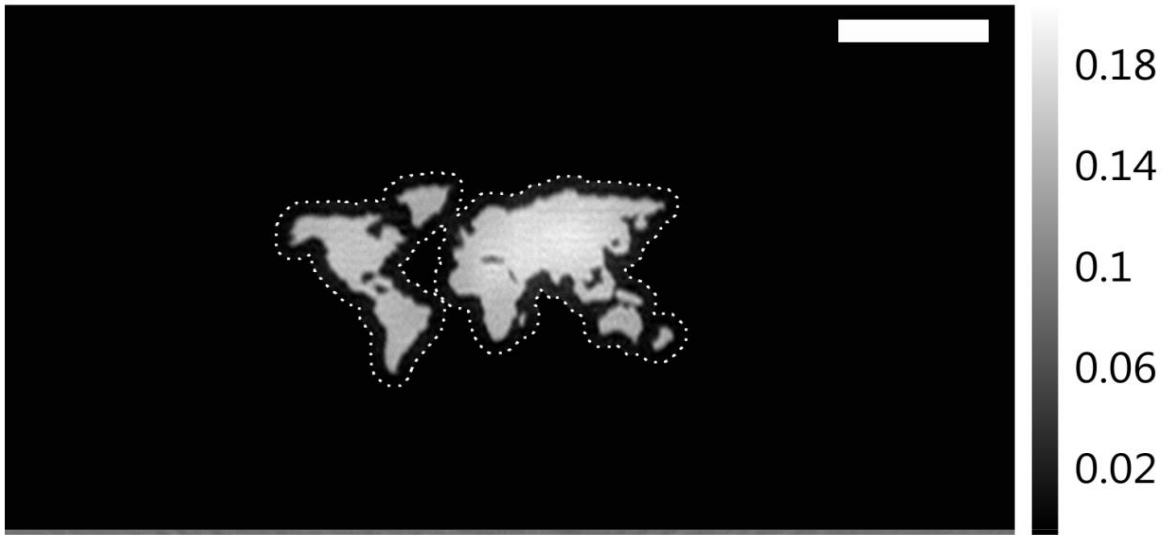

M. Bartels et al. Phys.Rev.Lett. 2015

bacteria *Deinococcus Radiodurans*

- **Among most radiationresistant organisms on earth, can survive 15 kGy of ionizing radiation**
- **very effective DNA repair mechanism,**
- **DNA packing debated**

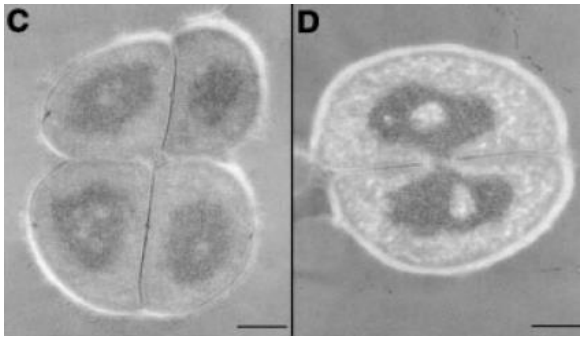

TEM-slices, Os-stained chromatin
Levin-Zaidman, Science (2003)

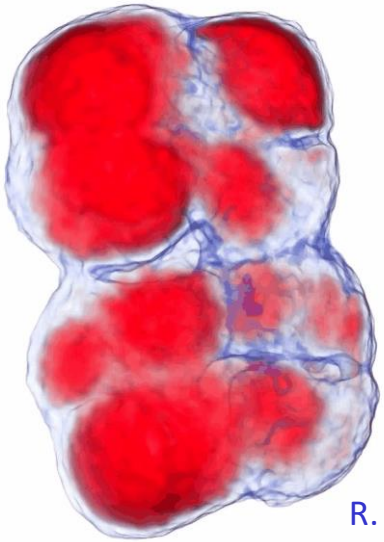

ptychography dose/projection: 1.5 10^6 Gy

R. Wilke et al., Opt. Express 2012

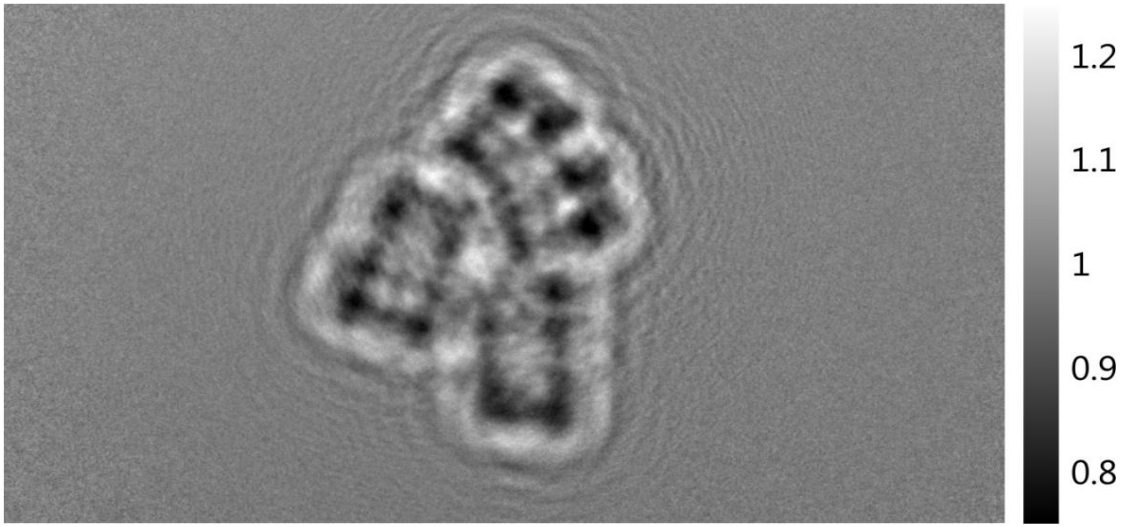

Waveguide: 2x10^9 ph/s, 20 nm x 17 nm, 7.9 keV
8 second dwell time 1920x1080 pixel sCMOS
20 nm pixel size

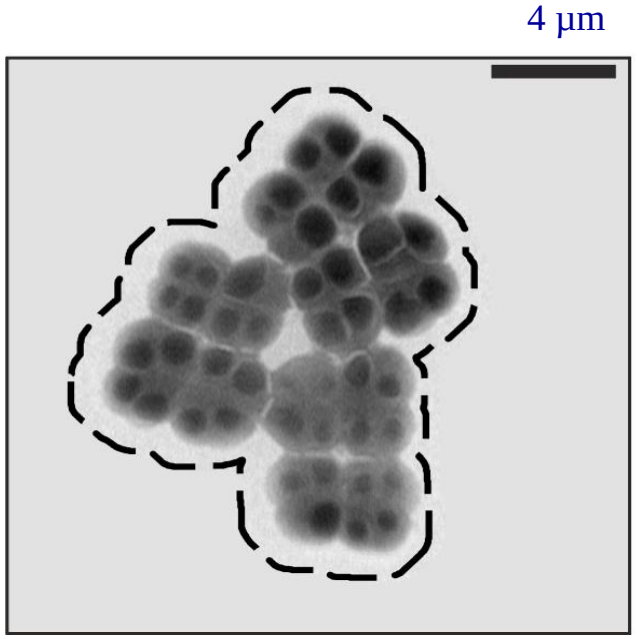

mHIO reconstruction

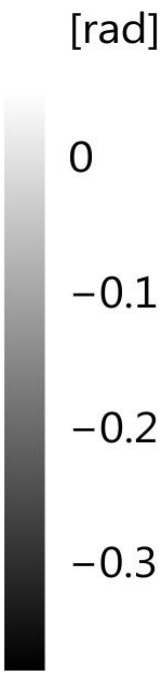

r=53 nm
5x10^3 Gy
7.9 keV

Low flux/dose rate:
5x10^5 ph/µm^2/s

dwell time: **8s**
Field of view: **20 µm x 20 µm**

M. Bartels et al. Phys.Rev.Lett. 2015

Living cells in cell culture chamber

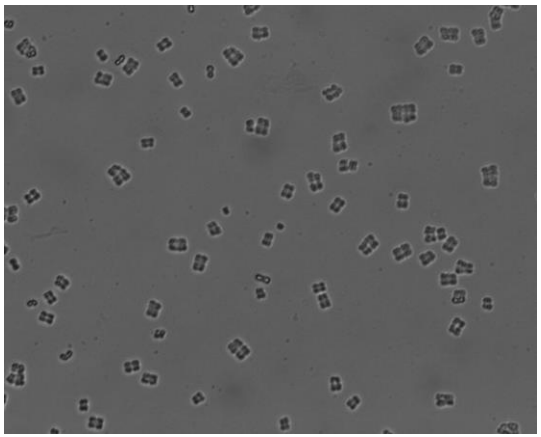

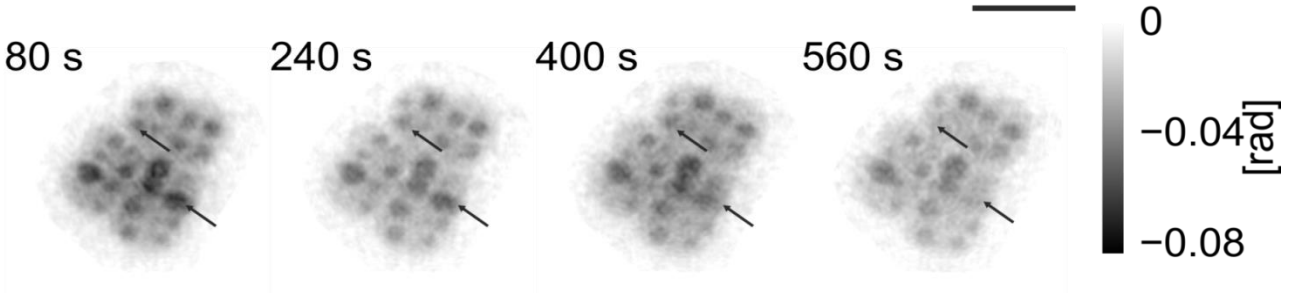

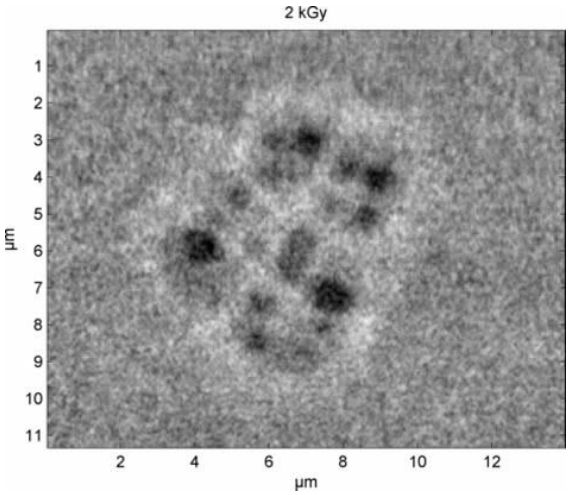

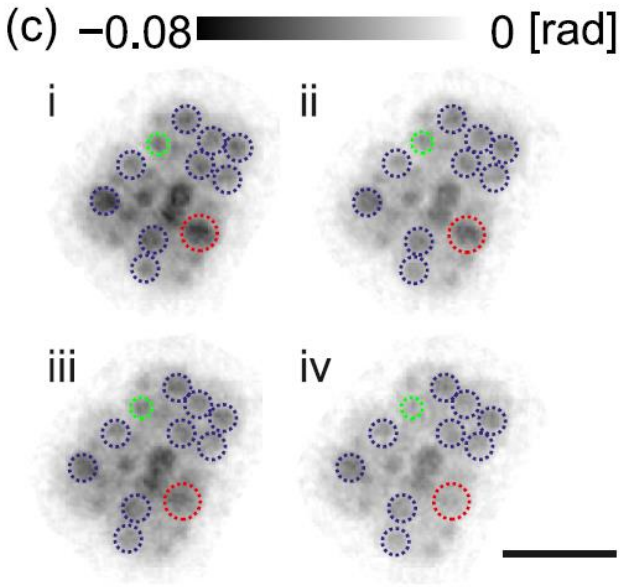

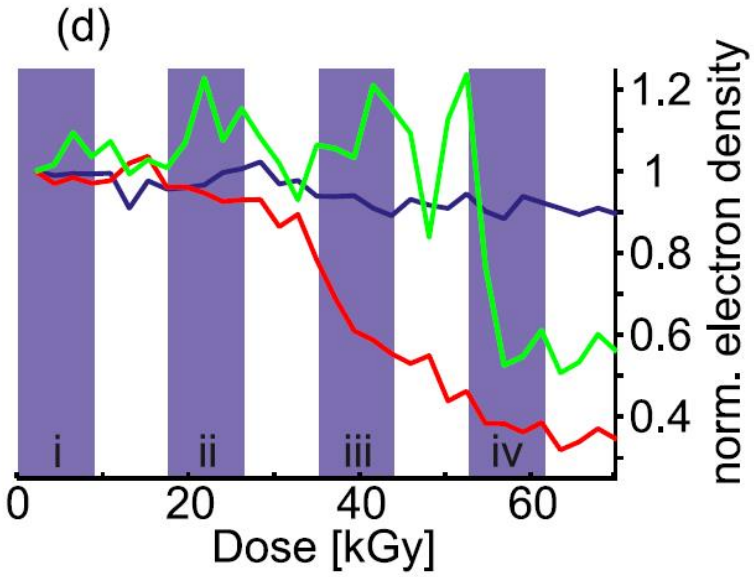

living cells in liquid chamber

radiation damage after

very long exposures

- each frame recorded for 80s

M. Bartels et. al. , Phys. Rev. Lett. 2015

Dose-resolution relationships

phantoms *NFH data* *CDI data*

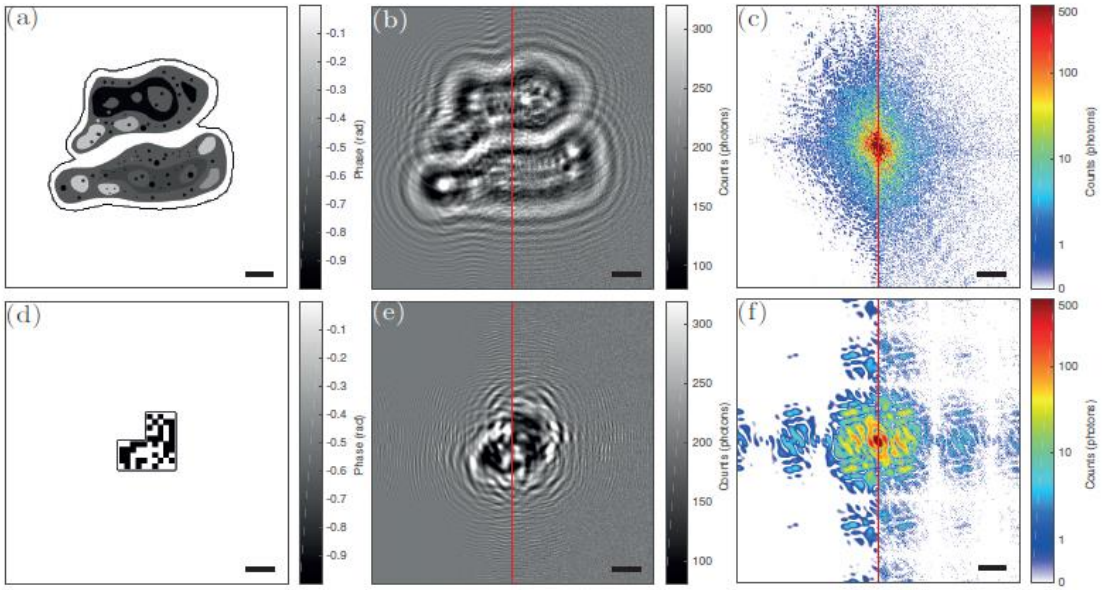

- *simulate noise with fluence μ [ph/pixel]*
- *reconstruct NFH and CDI under same constraints*
- *determine resolution by Fourier Shell Correlation*

-> ***NFH significantly more dose efficient***

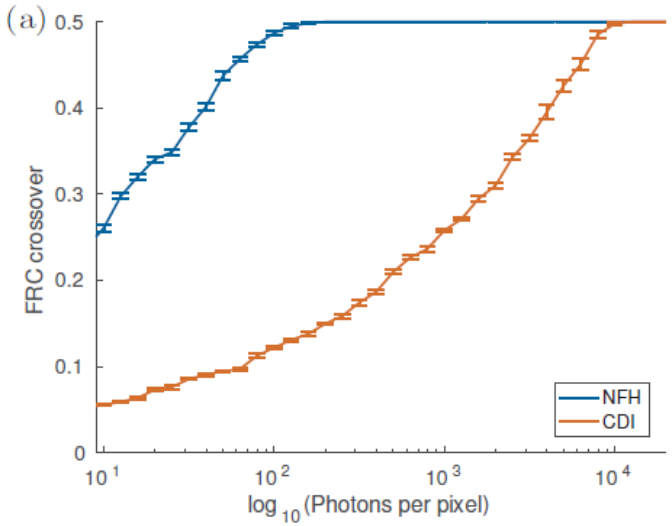

example: 200 ph/pixel

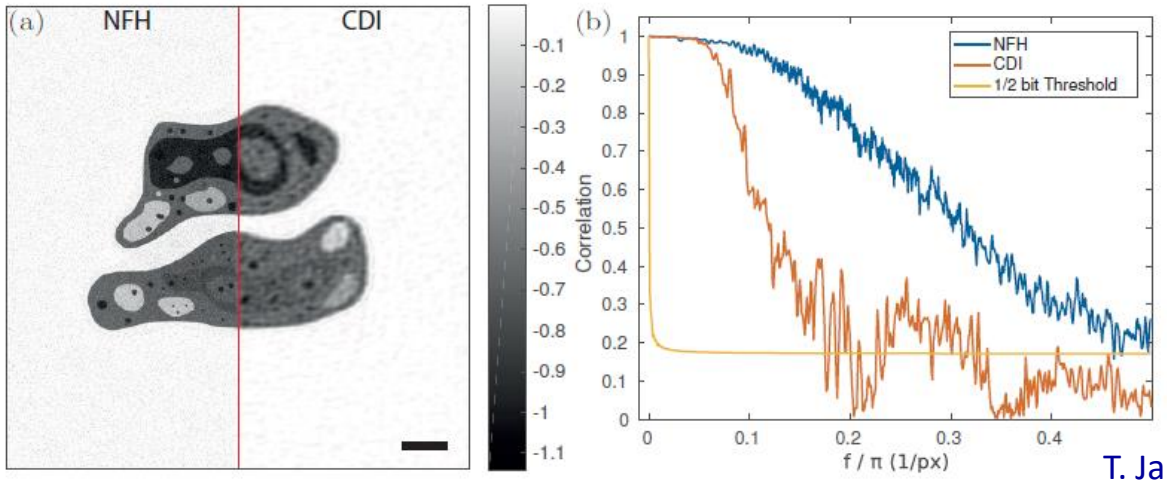

J. Hagemann, T. Salditt, J. Appl.Cryst. 2017
T. Jahn, R. Wilke, Y. Chuchkin, T. Salditt, Acta Cryst A 2017

Tomography of a macrophage (after lunch)

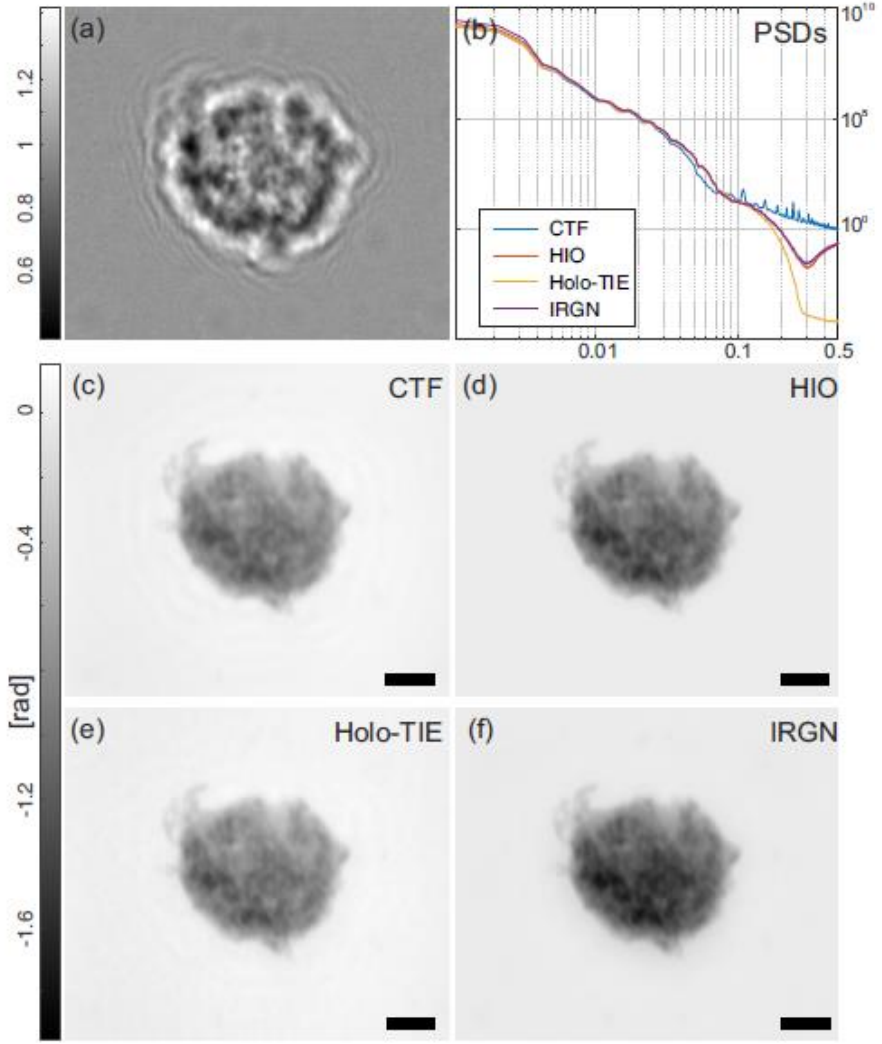

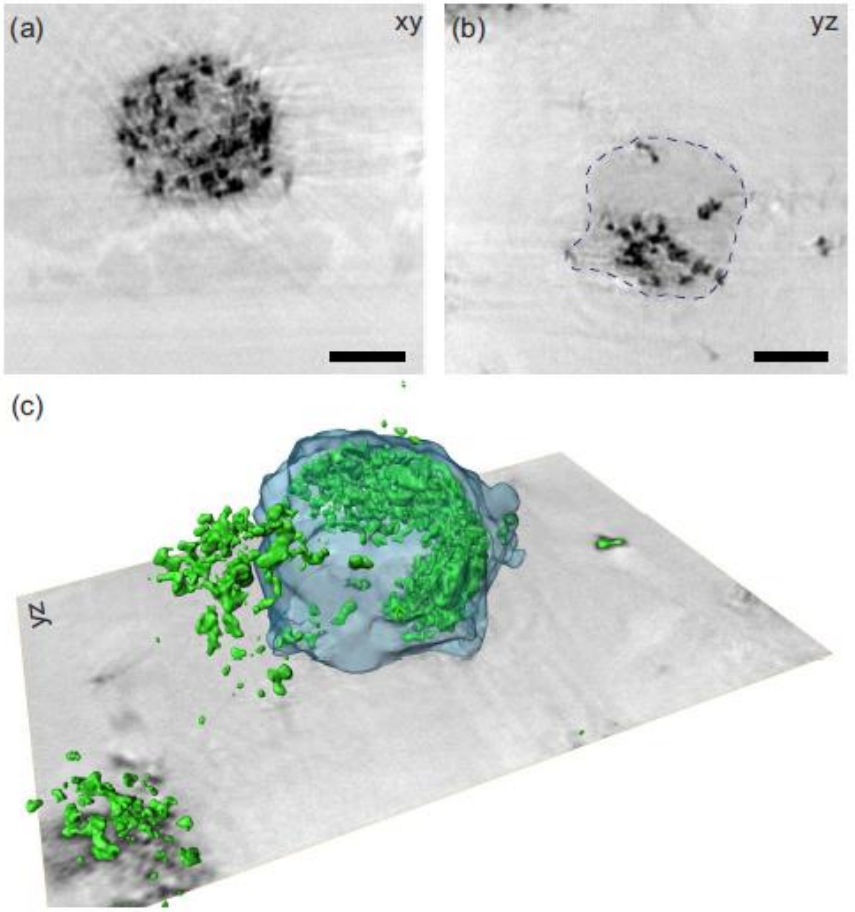

Optimized phase retrieval
M. Krenkel et al., Acta Cryst., 2017

Cells in functional environment: macrophages in lung tissue

blood vesells (purple)

barium (green)

soft tissue (yellow)

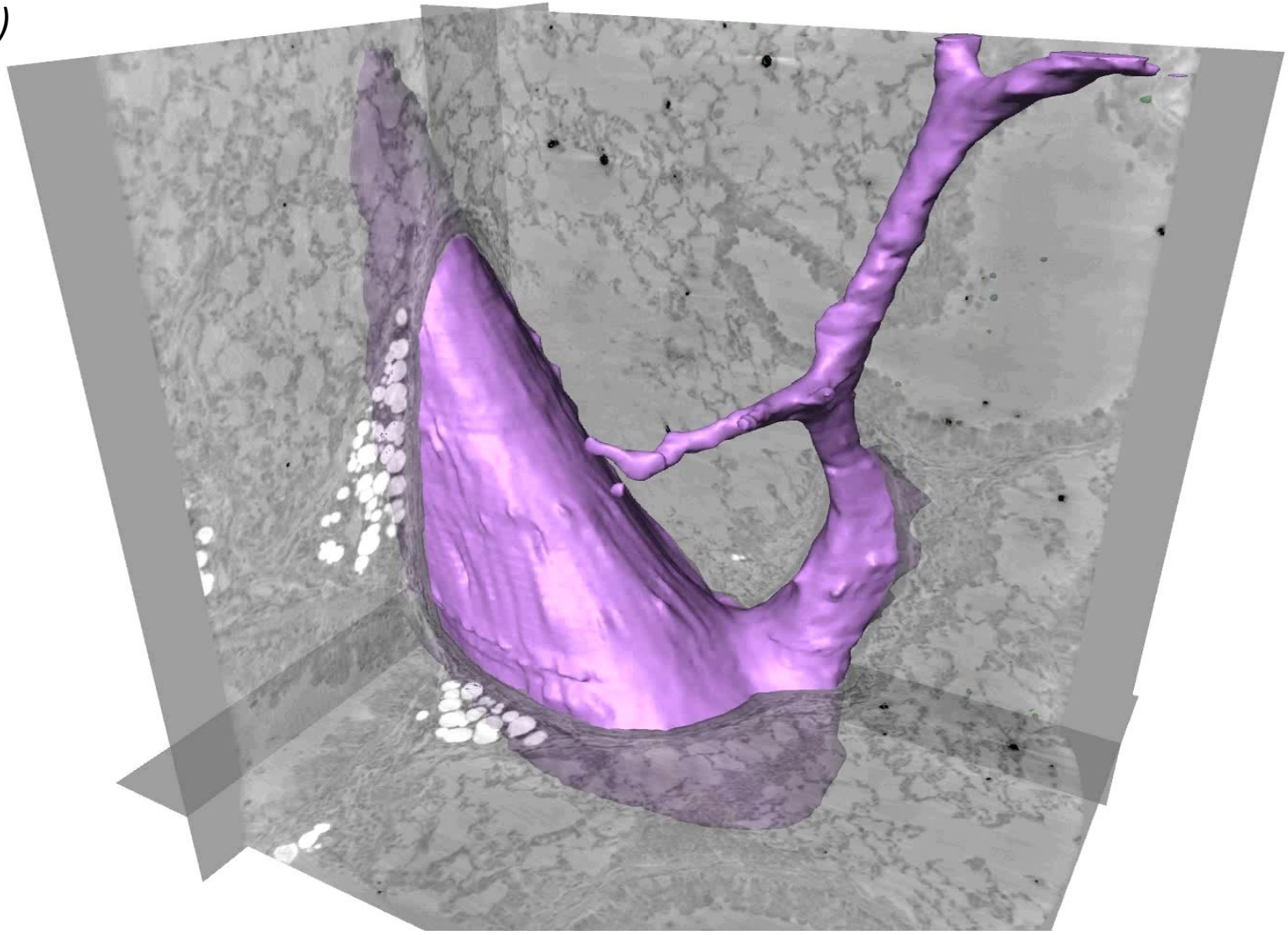

Martin Krenkel et al., Sci.Rep. 2015

ID22Ni, 17.5keV – small magnificationm 470 nm voxel
lung (WT mouse, no astma)

To higher resolution

holographic projection of
lung tissue slice in WG beam

zoom to ROI by moving
closer to the focus

CTF based phase retrieval (1 or multiple distances)

region of interest tomography

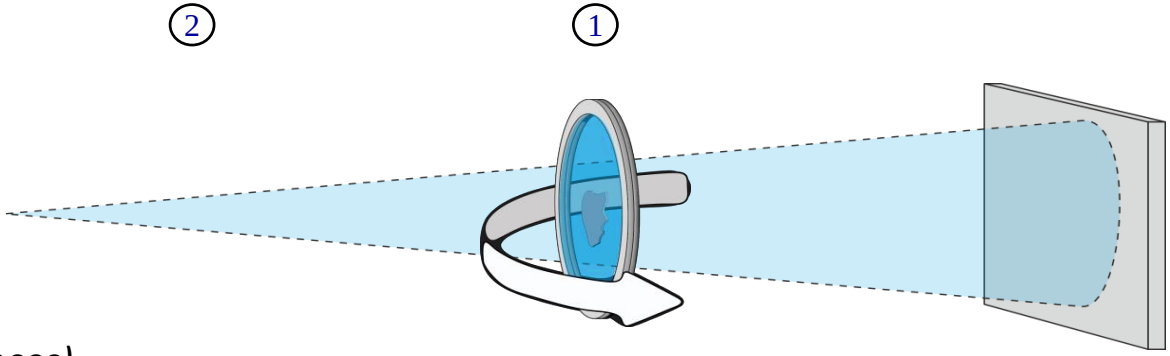

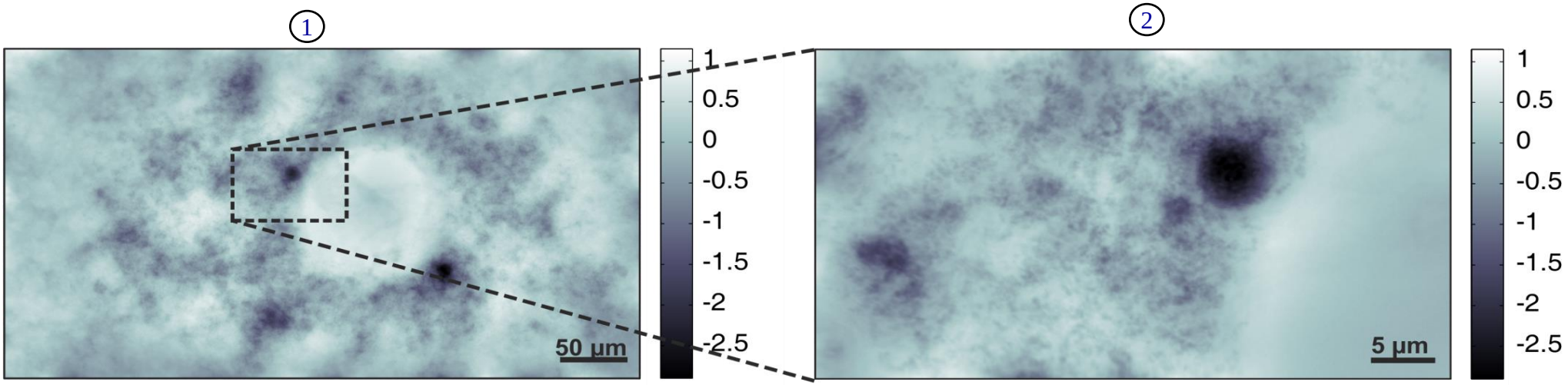

blood vessel / barium / bronchial walls (yellow) / single cell

lung tissue (mouse), 13.8keV , 50 nm voxel

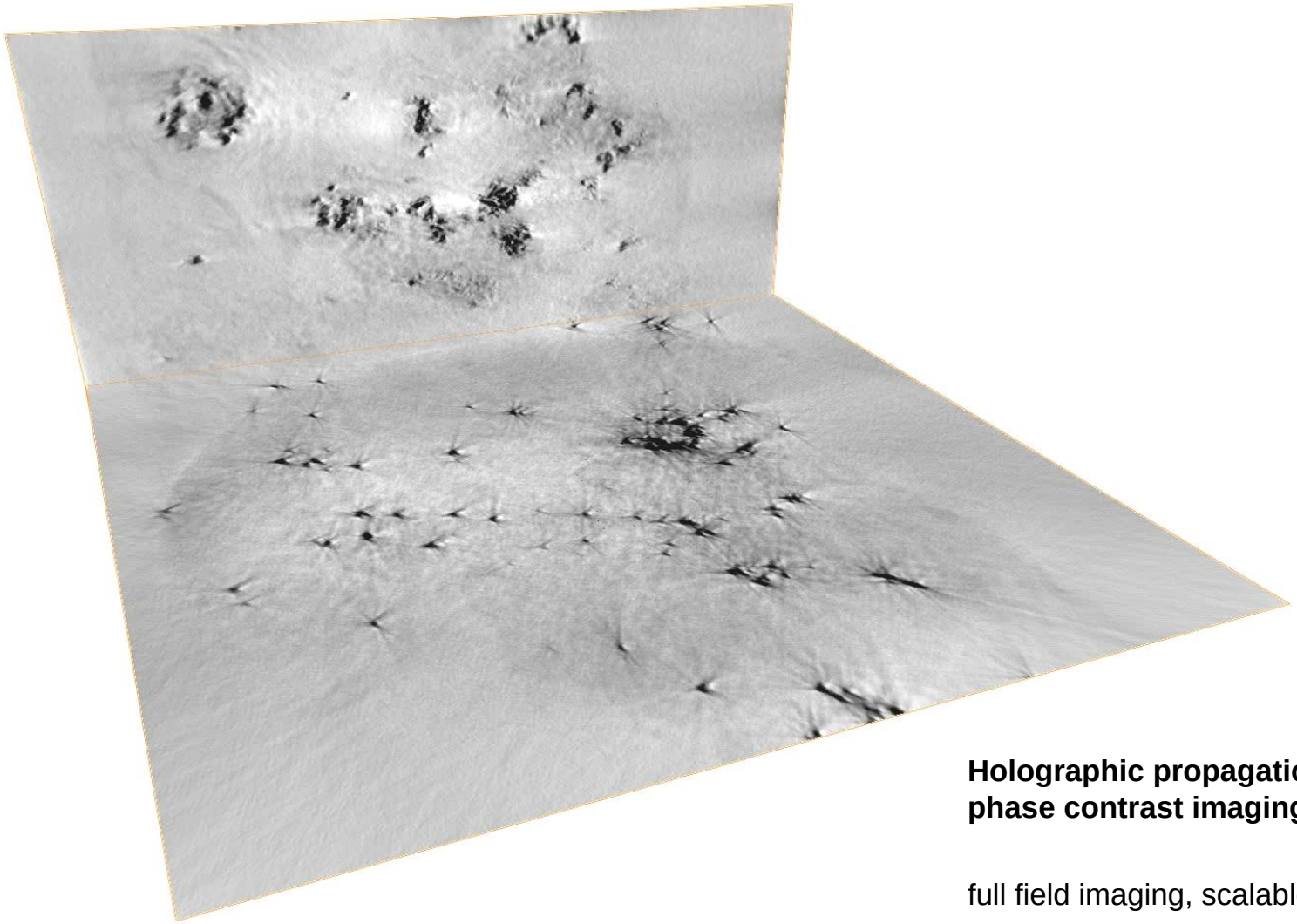

Holographic propagation based phase contrast imaging

full field imaging, scalable resolution & FOV

zoom-tomography: -> native hydrated soft tissue

-> sub-cellular resolution in large tissue in 3D

Göttingen Instrument for Nano-Imaging with X-rays (GINIX) @ Petra III / Desy

Martin Krenkel et al., Sci.Rep. 2015

Advanced near-field tomography: simultaneous phase retrieval and 3D reconstruction

- *standard tomography based on the 2D Radon transform*
- *for finite object different slices (projections) are not independent*
- *in near field different planes are also coupled, (x,y,z_1) & (x,y,z_2)*

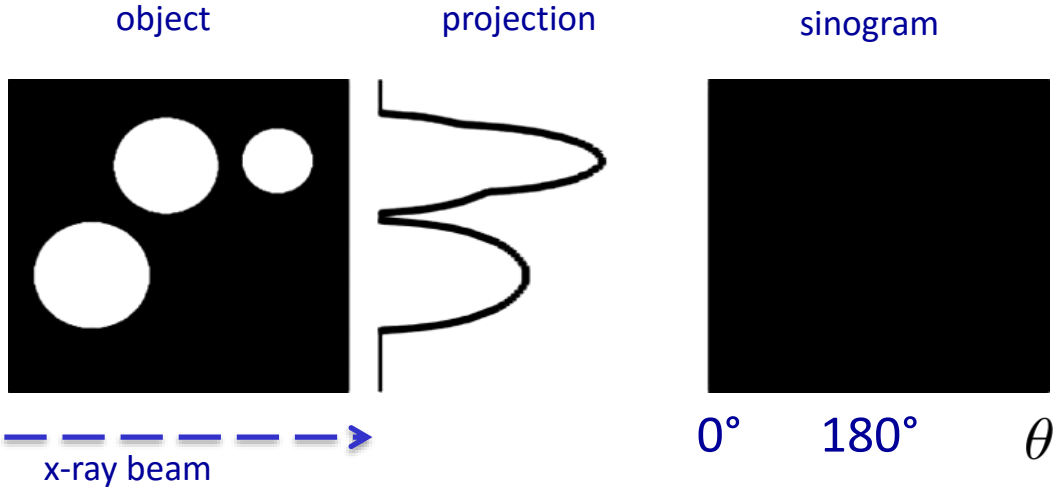

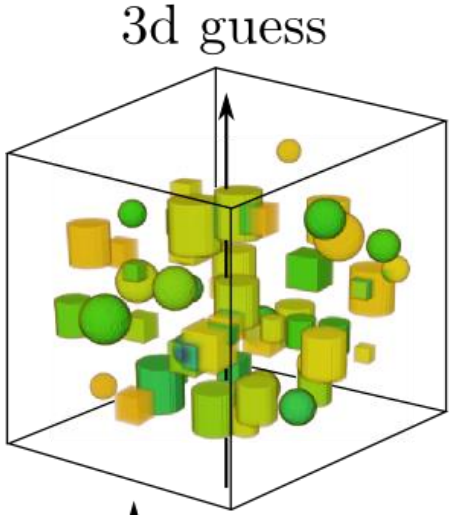

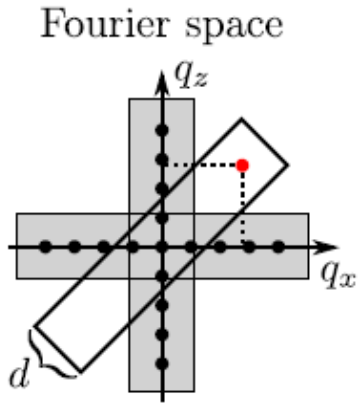

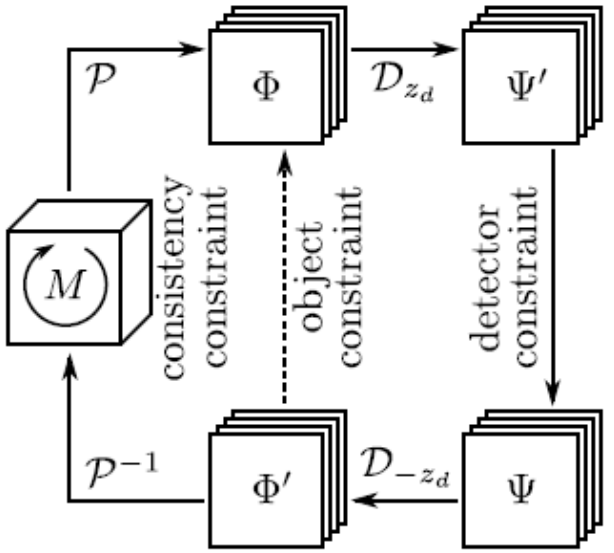

- *Helgason-Ludwig consistency conditions*
- *reconstruct „all in once“*
- *implement as ART*
- *3D stabilizes phase retrieval*
- *overcomes need for a prioris & linerisations*

Iterative reprojection phase retrieval (IRP)

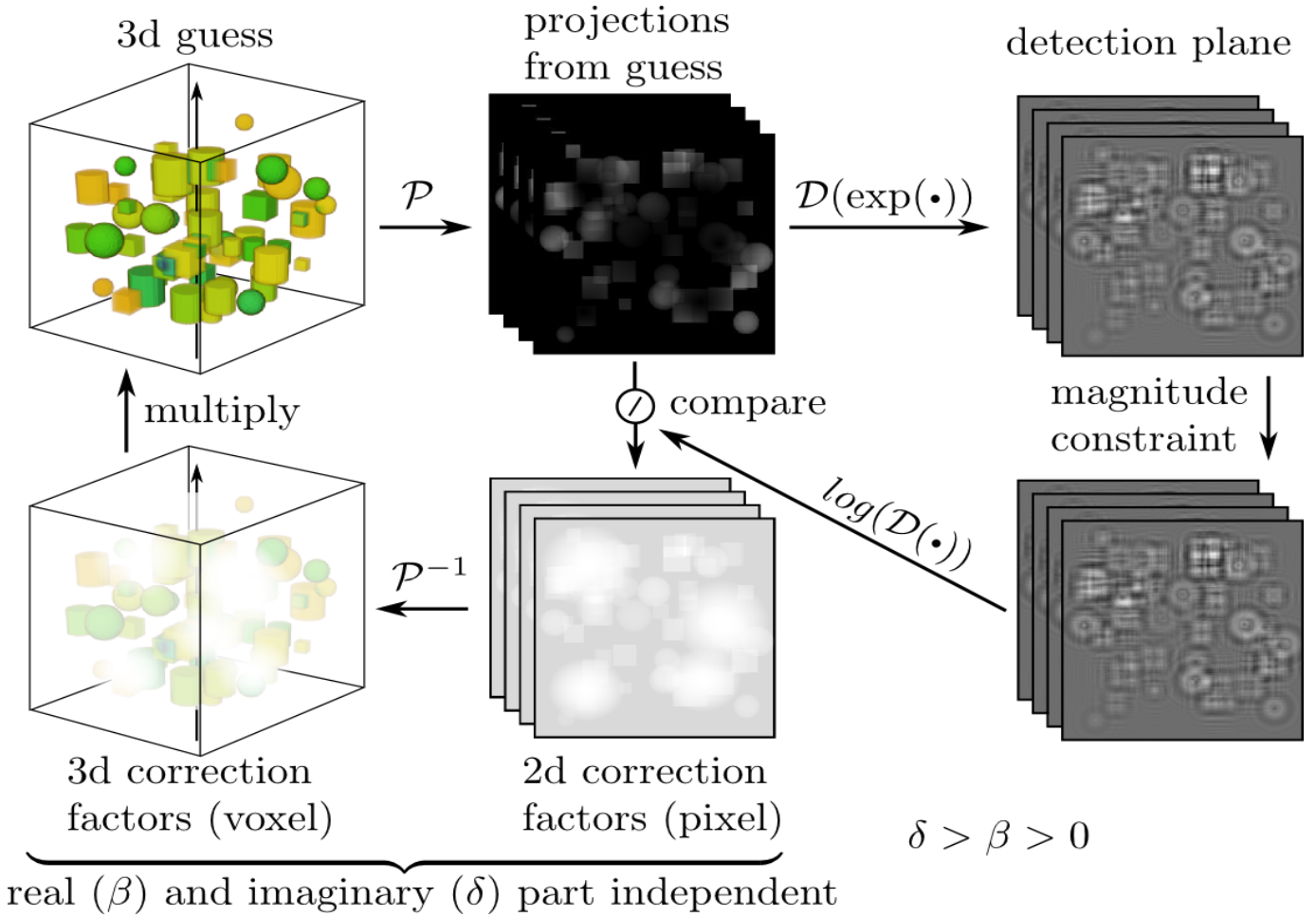

$$\Omega_{n+1} = \frac{\Omega_n}{N} \cdot \sum_\alpha \left(\mathcal{P}_\alpha^{-1} \frac{\Phi_\alpha}{\mathcal{P}_\alpha(\Omega_n)} \right)$$

Ruhlandt et al. Phys.Rev.A 89, 033847 (2014)

The benefit of tomography for phase retrieval

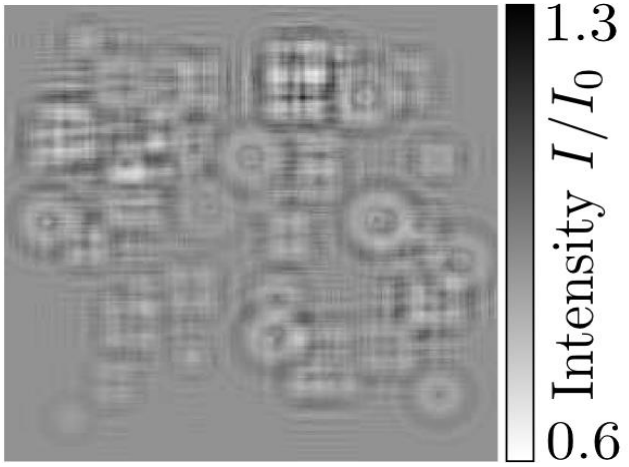

F= 0.01,256 x 256 px, 1000 it.
different materials , $\beta/\delta \in [0...0.15]$

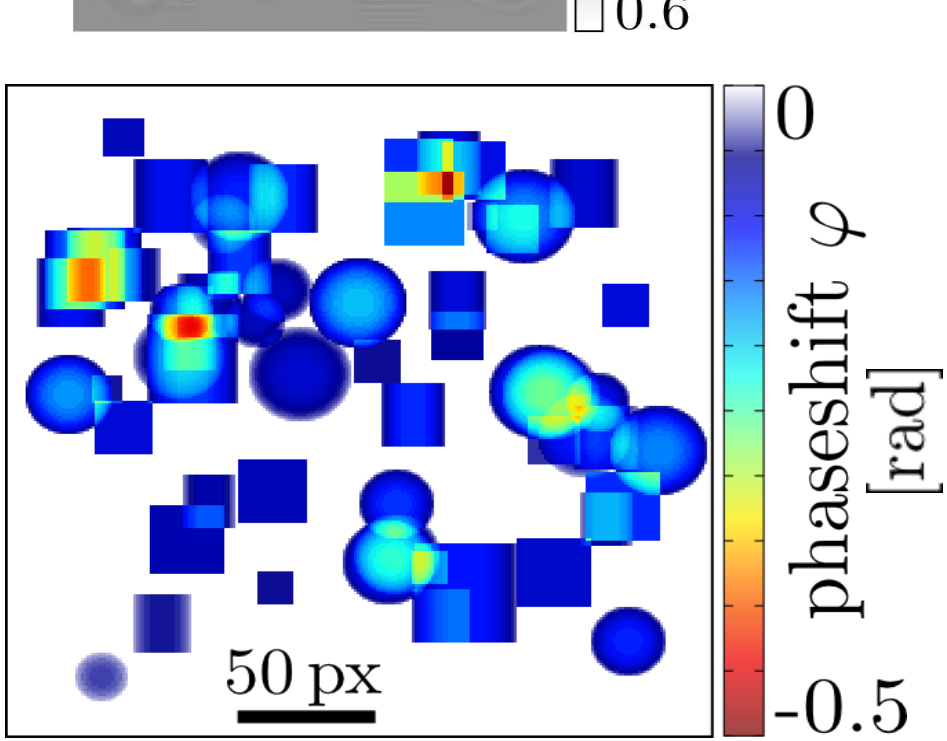

$N = 128$

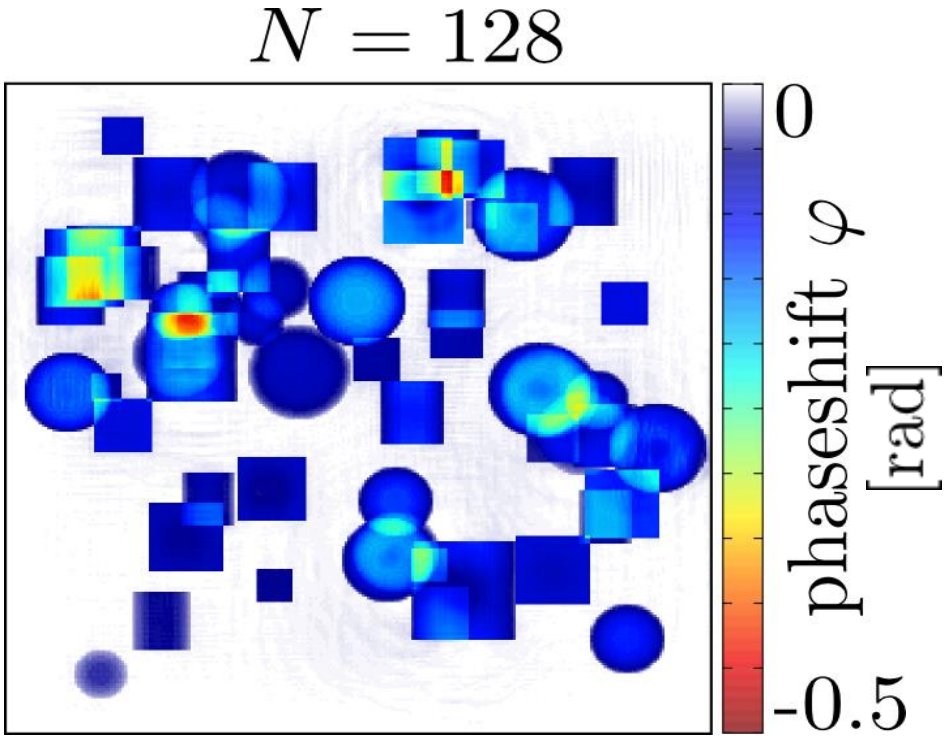

Ruhlandt et al. Phys.Rev.A 89, 033847 (2014)

II.
3d histology of neuronal tissue:

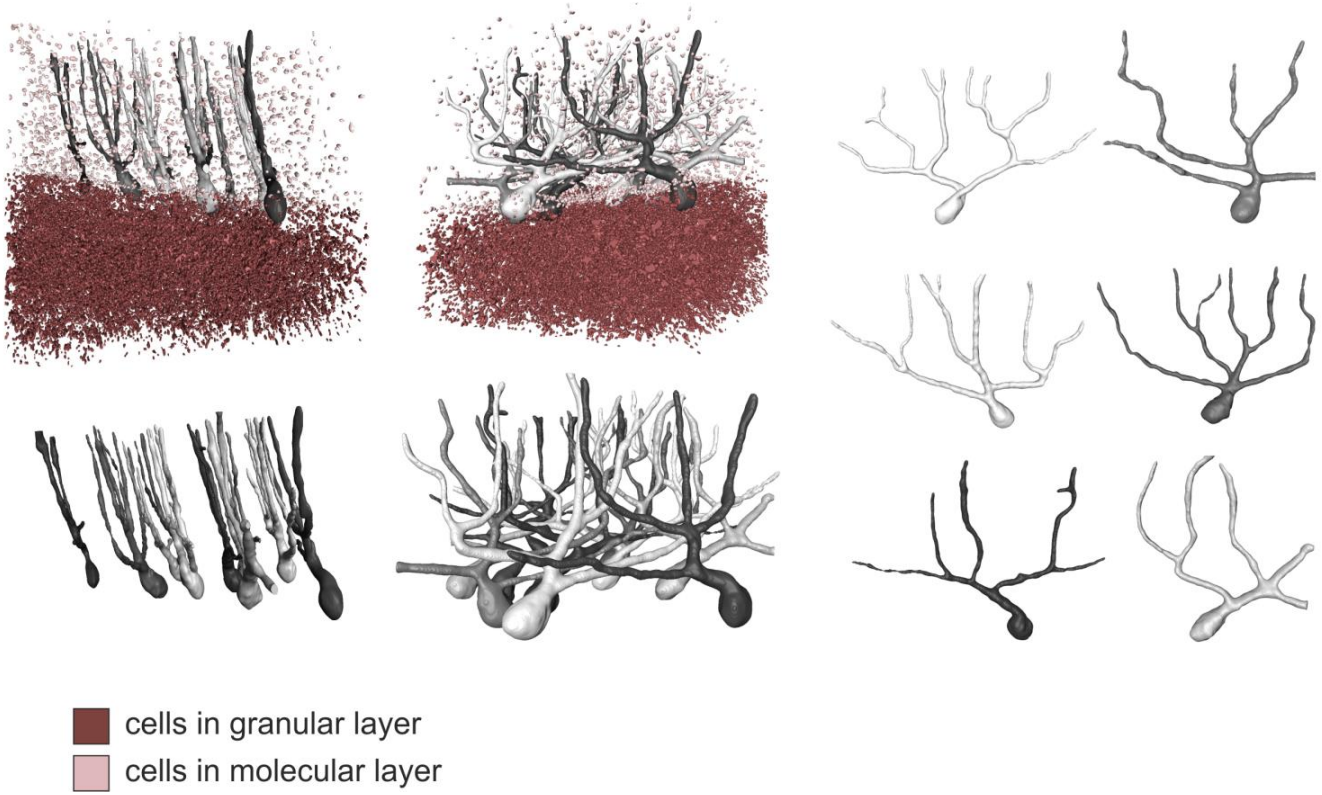

Mareike Töpperwien

mouse retina

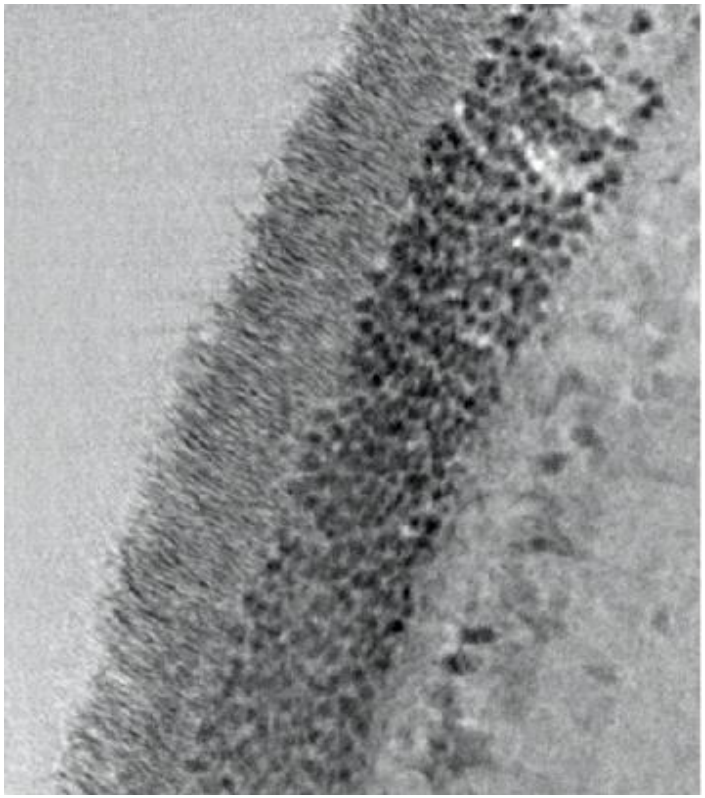

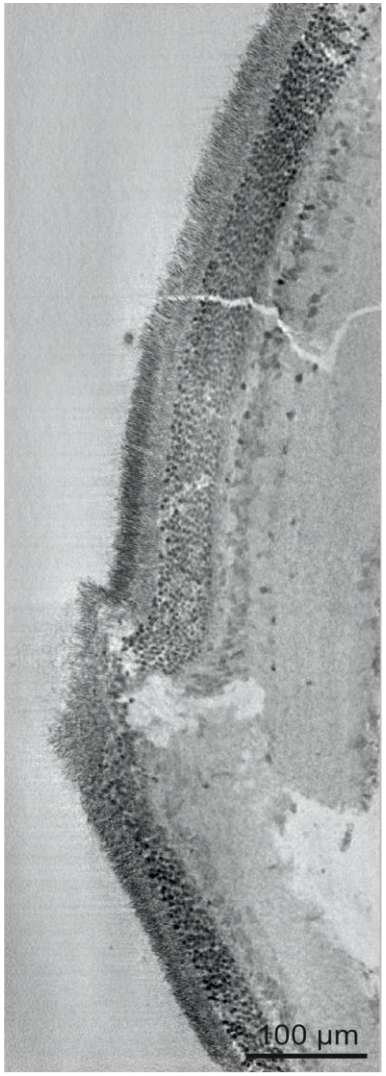

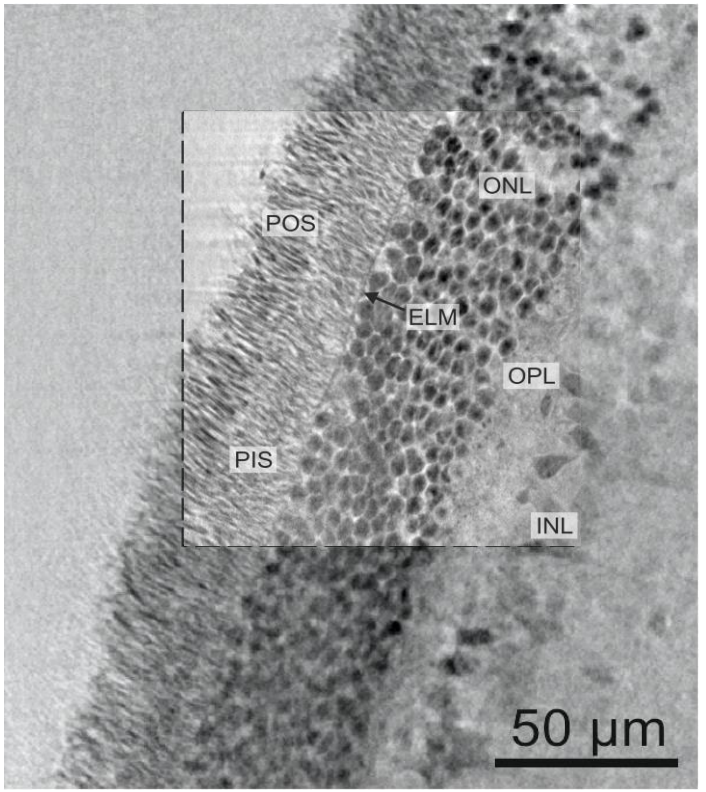

‘low resolution’-tomography

- effective pixel size: 182 nm
- 13.8 keV, 1 distance
- 900 projections, 1 s exp. time

Zoom-tomography

- effective pixel size: 63 nm
- 13.8 keV, 4 distances
- 900 projections, 1 s exp. time

Mareike Töpperwien et al., unpublished

mouse brain biopsy (paraffin) / unstained

- 1 mm biopsy punch from unstained mouse brain in paraffin (region: cerebellum)
- effective pixel size: 186 nm
- 8 keV, 4 distances
- 1500 projections, 0.1 s exp. time

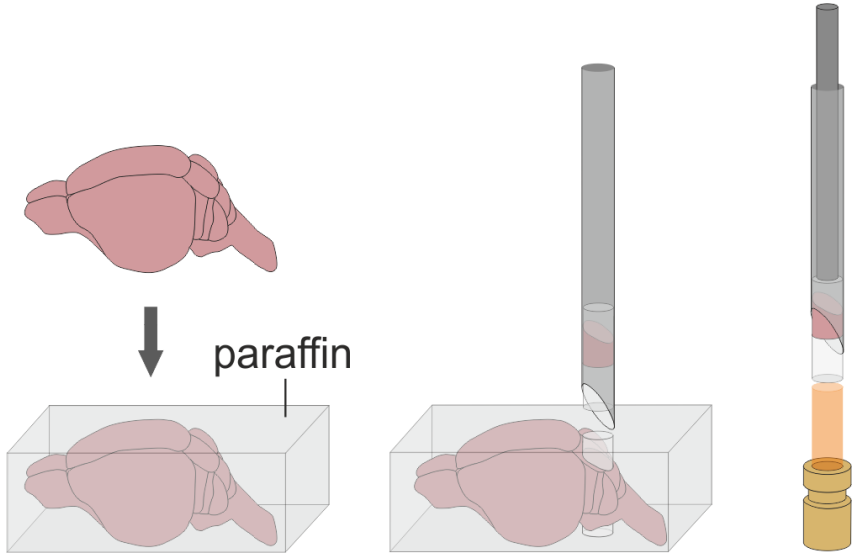

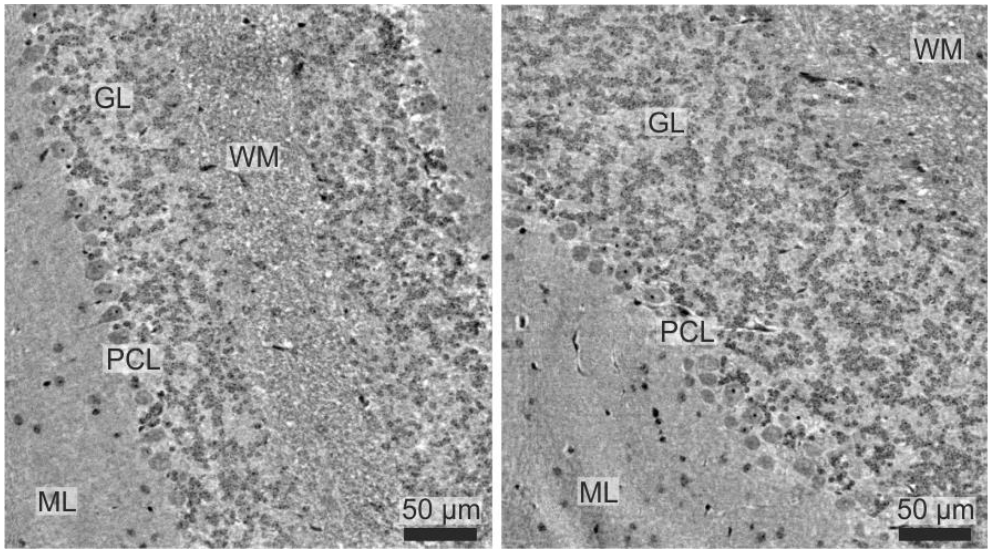

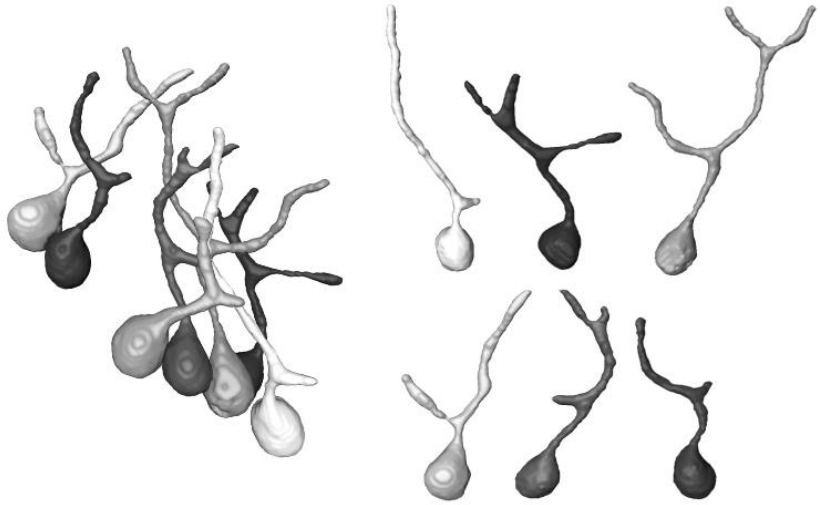

Mareike Töpperwien et al., unpublished

human cerebellum in paraffin / unstained

1 mm biopsy punch

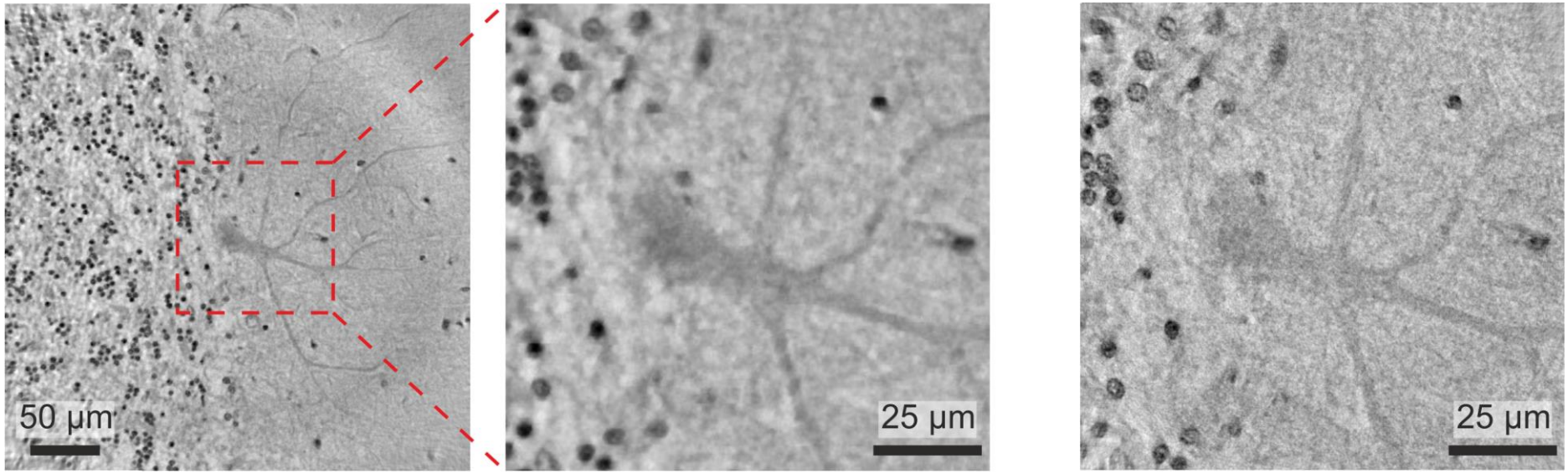

‘low resolution’-tomography

- effective pixel size: 186 nm
- 8 keV, 4 distances
- 1500 proj., 0.05 s exp. time

Zoom-tomography

- effective pixel size: 65 nm
- 8 keV, 4 distances
- 1500 projs., 0.05 s exp. time

Mareike Töpperwien et al., unpublished

3d Histology: unstained human cerebellum

- 1 mm biopsy punch from unstained brain of mouse/human cerebellum
- paraffin embedded or in ethanol
- effective pixel size: 186 nm / zoom: 65nm
- 8 keV, 4 distances
- 1500 projections, 0.05 s exp. time

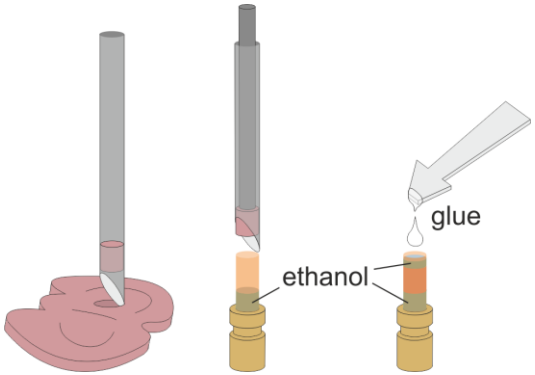

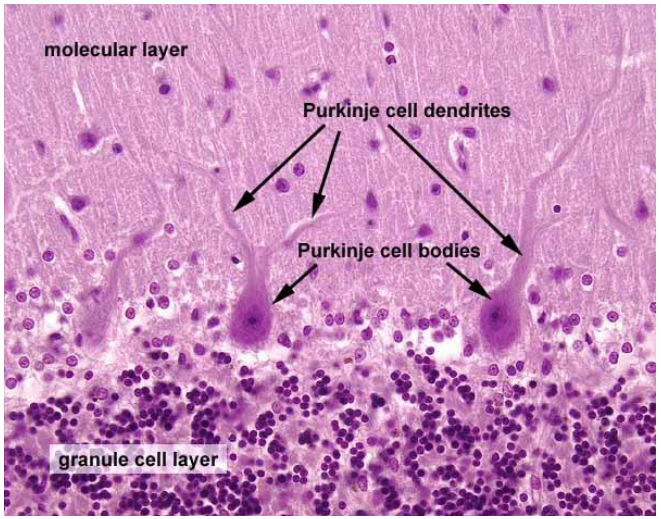

http://www.siumed.edu/~dking2/ssb/NM031b.htm

human/ paraffin embedded

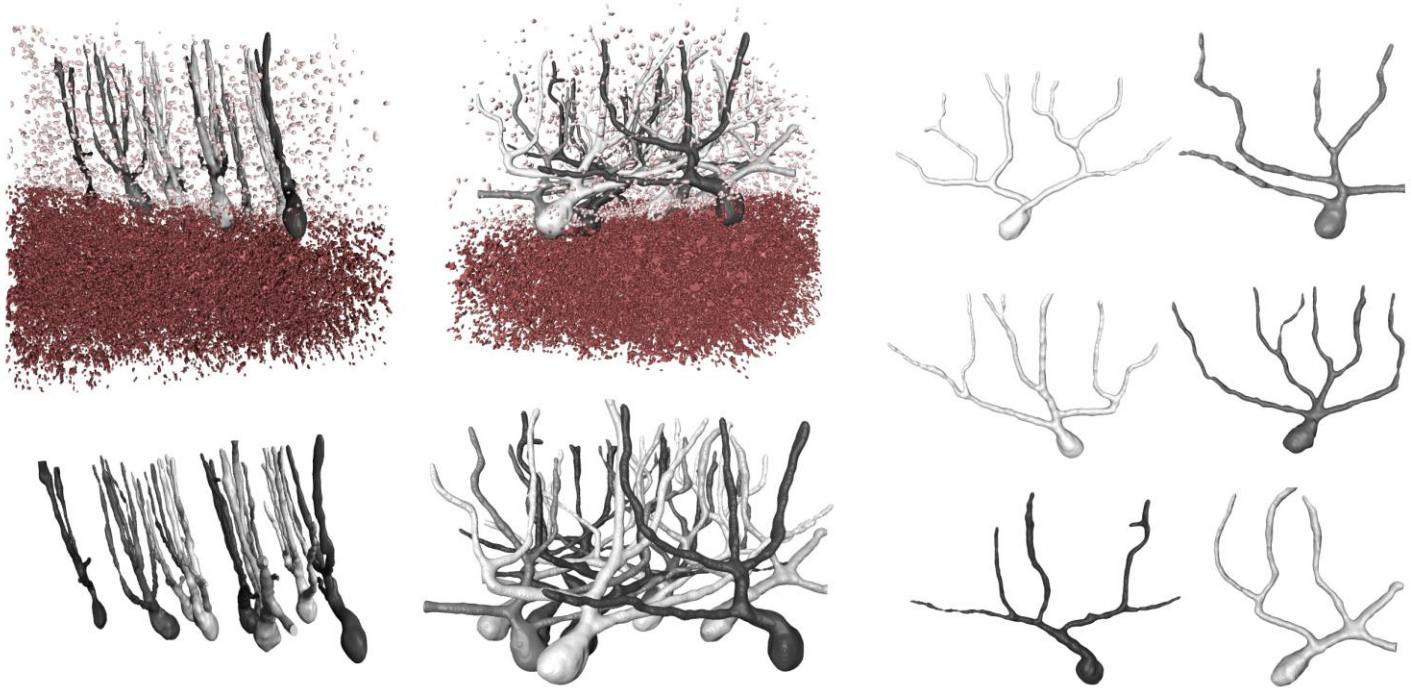

- histology:

  fixation
  dehydration,
  clearing
  impregnation
  embedding,
  sectioning
  slide staining

cells in granular layer
cells in molecular layer

Töpperwien et al., unpublished

Unstained human cerebellum in paraffin

- 1 mm biopsy punch from human cerebellum in paraffin
- effective pixel size: 0.46 µm
- 1000 projections, 50 s exp. time

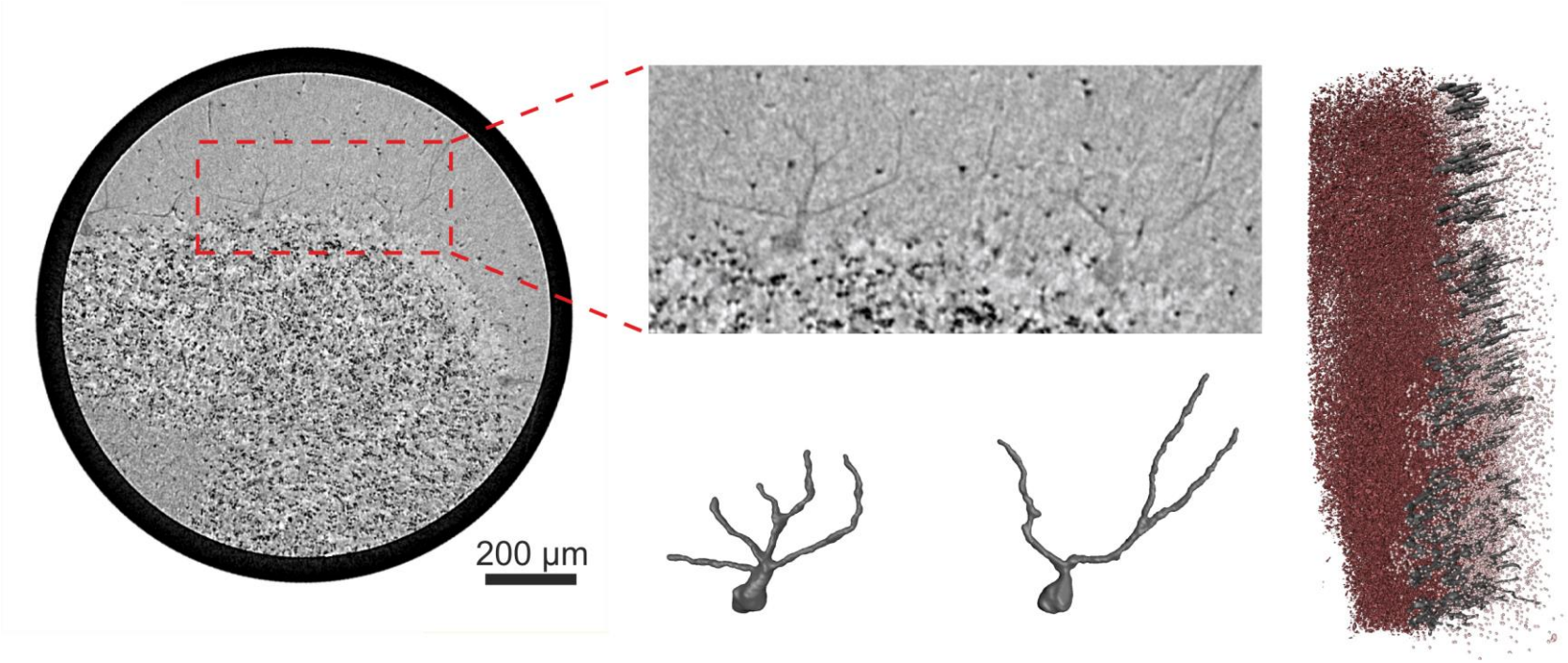

Töpperwien et al., unpublished

quantitative analysis of granular cell correlations

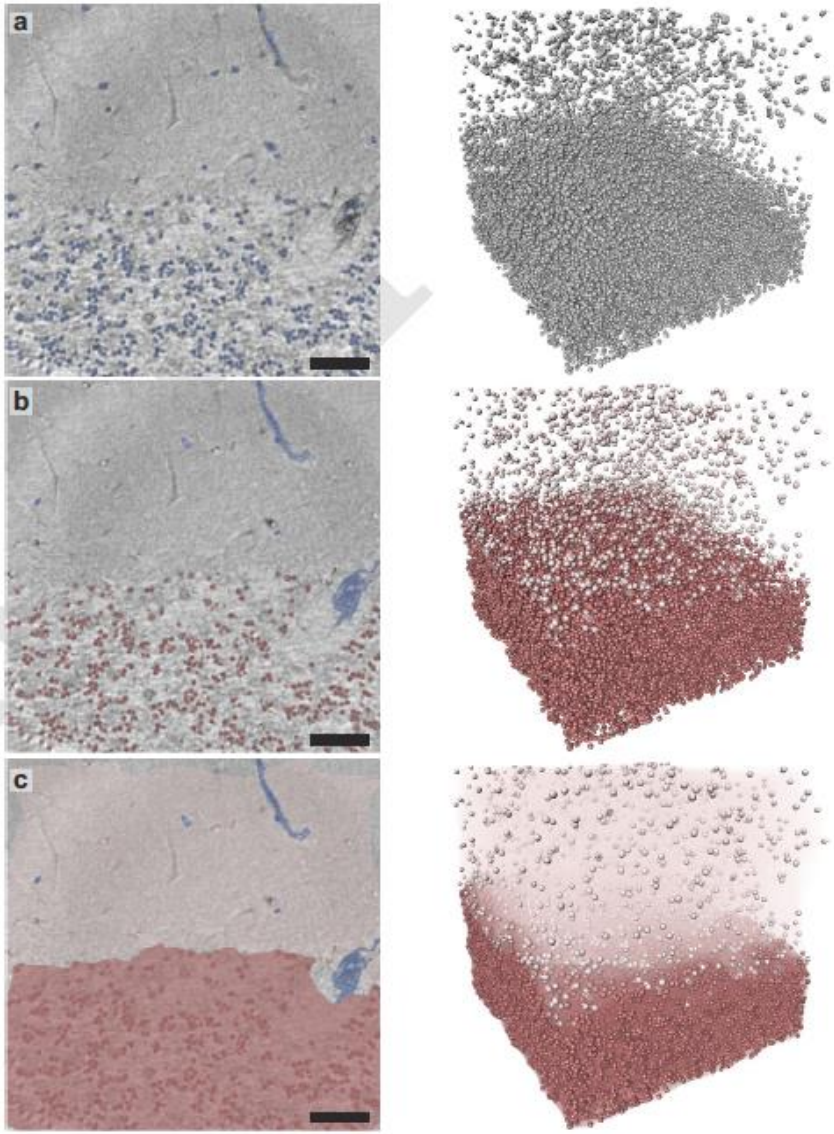

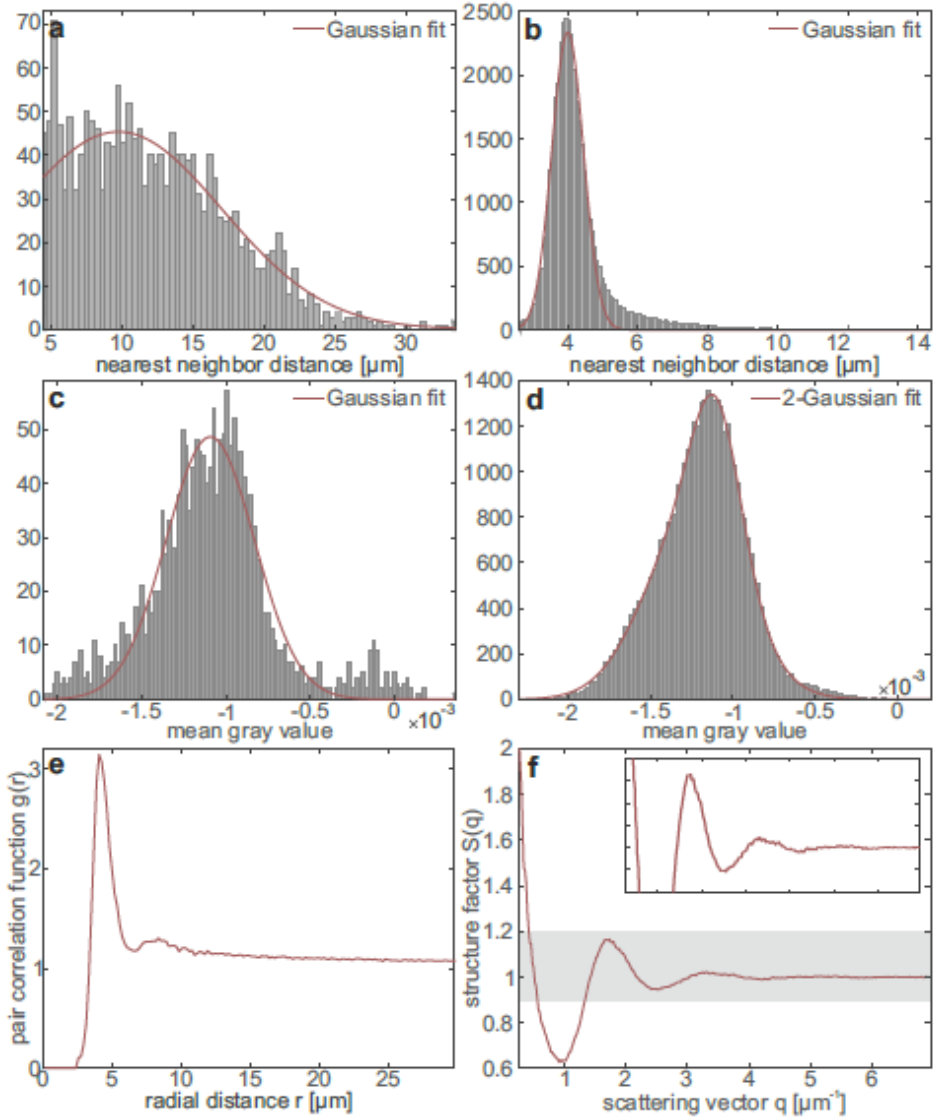

Fig. 3. Results of the automated segmentation procedure. (a,b) Overlay of all cells detected by the algorithm based on the Hough transform on the corresponding reconstructed virtual slice as well as a volume rendering indicating their spatial distribution. (c,d) Result after manual removal of blood vessels and division into molecular layer (light red) and granular layer (dark red) based on the mean distance to the 35 nearest neighbors of each cell. (e,f) Volume estimation for each layer used for calculating the cell densities. Scalebars: 50 µm

III.
dynamic tomography: towards 4d movies at the nanoscale

Aike Ruhlandt

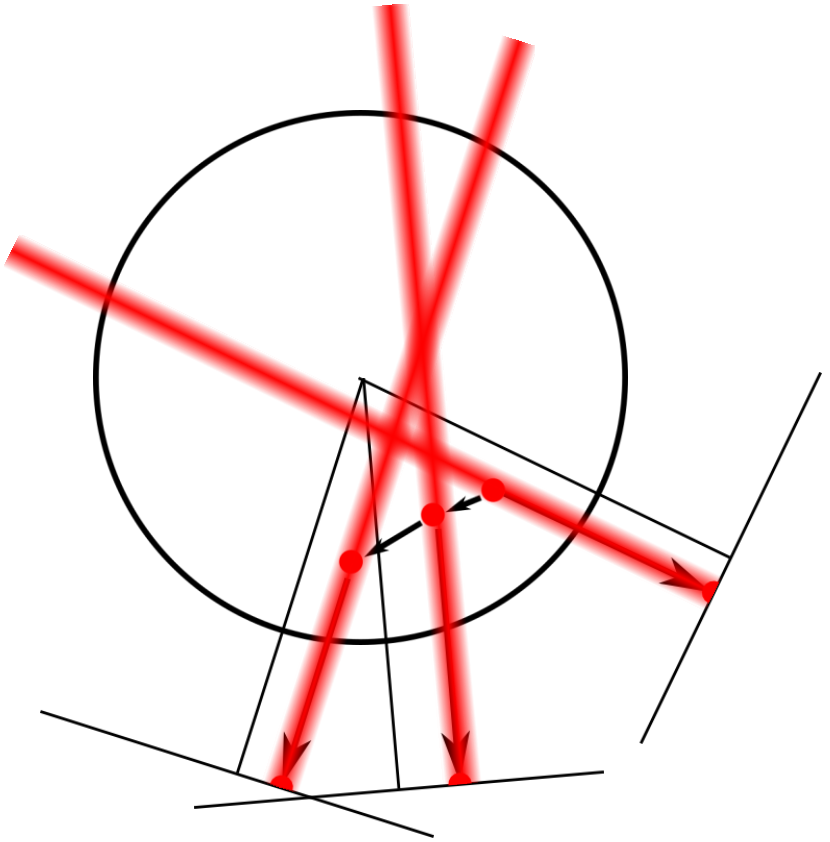

measure fast !

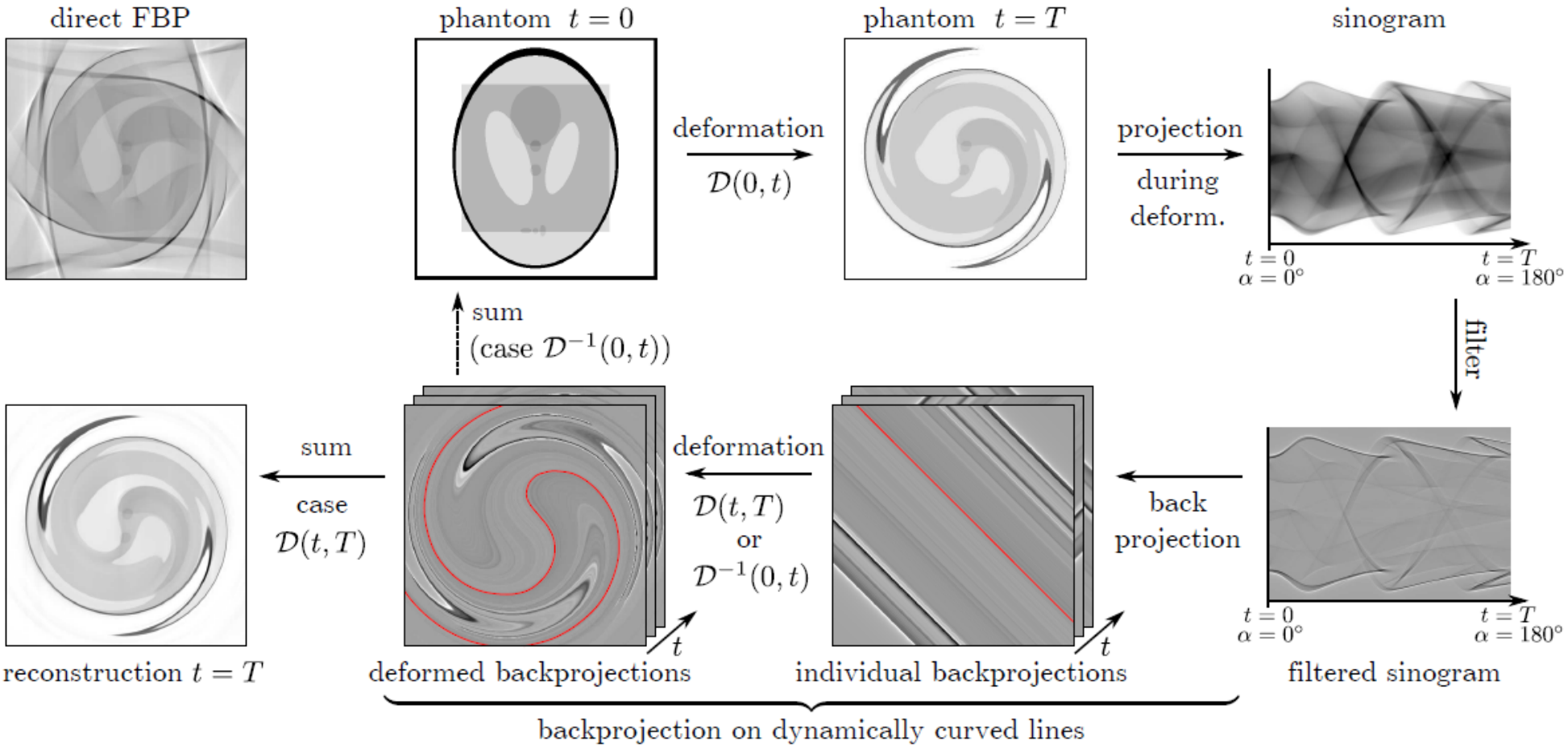

Ruhlandt, A.; Töpperwien, M.; Krenkel, M.; Mokso, R. & Salditt, T.:
Four dimensional material movies: High speed phase-contrast tomography by backprojection along dynamically curved paths
Scientific Reports 7 (2017)

time-resolved phase contrast tomography: burning match

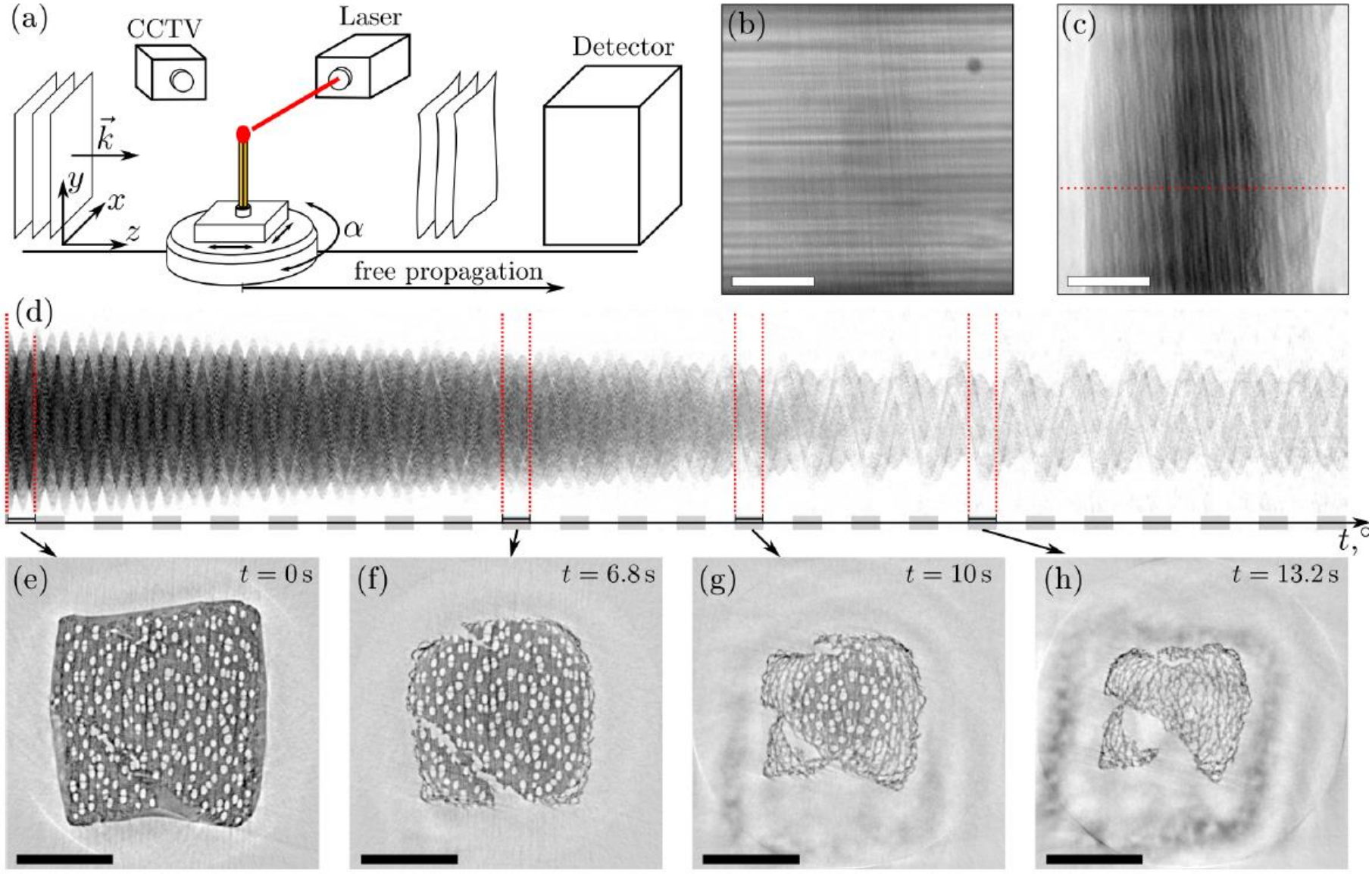

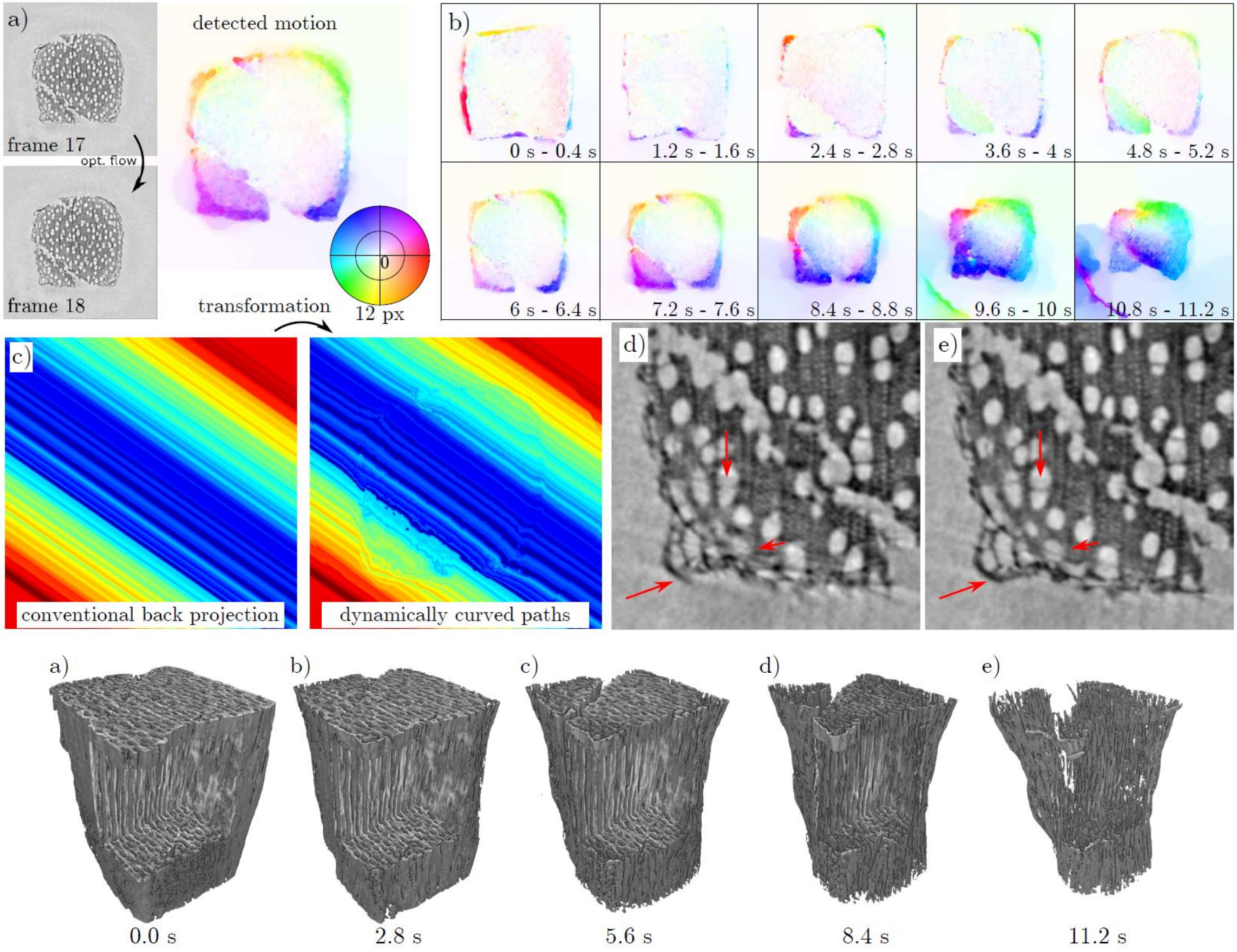
a)
frame 17
opt. flow
frame 18
detected motion
0
transformation
12 px
b)
0 s - 0.4 s
1.2 s - 1.6 s
2.4 s - 2.8 s
3.6 s - 4 s
4.8 s - 5.2 s
6 s - 6.4 s
7.2 s - 7.6 s
8.4 s - 8.8 s
9.6 s - 10 s
10.8 s - 11.2 s
c)
conventional back projection
dynamically curved paths
d)
e)
a)
0.0 s
b)
2.8 s
c)
5.6 s
d)
8.4 s
e)
11.2 s

rotation 1.25 Hz, 2.5 tomograms/sec , 1msec /projection, 18800 frames, voxel 2.95µm

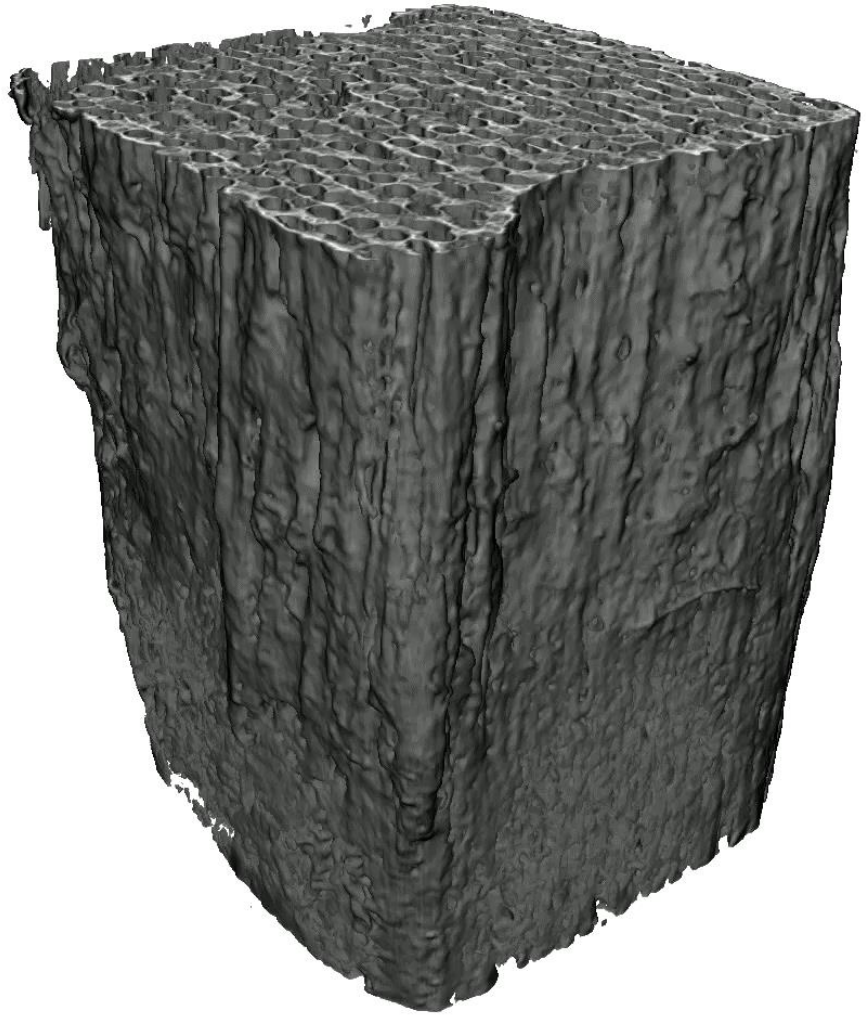

Ruhlandt, A.; Töpperwien, M.; Krenkel, M.; Mokso, R. & Salditt, T.:
Four dimensional material movies: High speed phase-contrast tomography by backprojection along dynamically curved paths
Scientific Reports 7 (2017)

Time-resolved tomography of colloidal diffusion & sedimentation

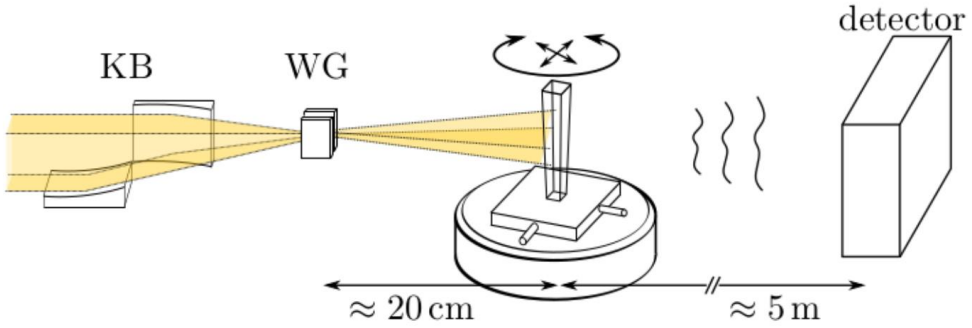

Göttingen instrument for nanoscale imaging with X-rays (GINIX)
@ beamline P10, DESY, Hamburg

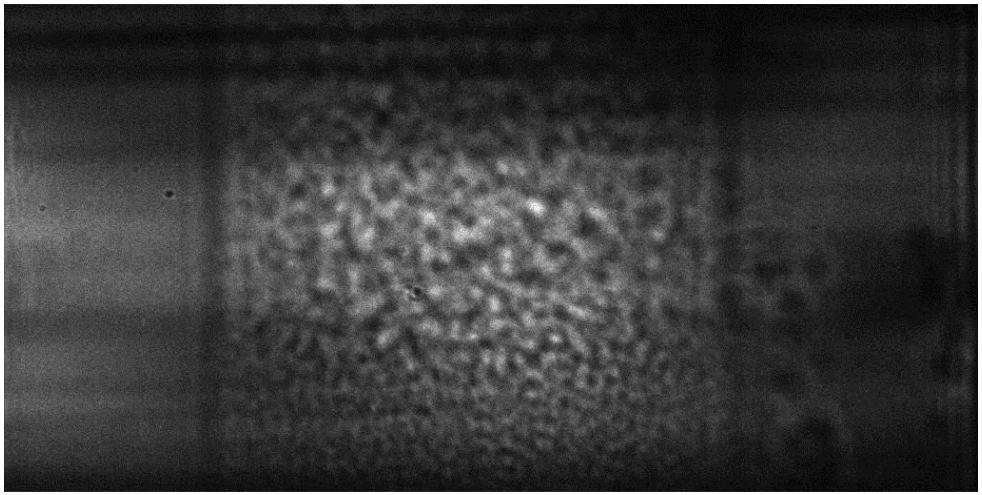

projections (raw)

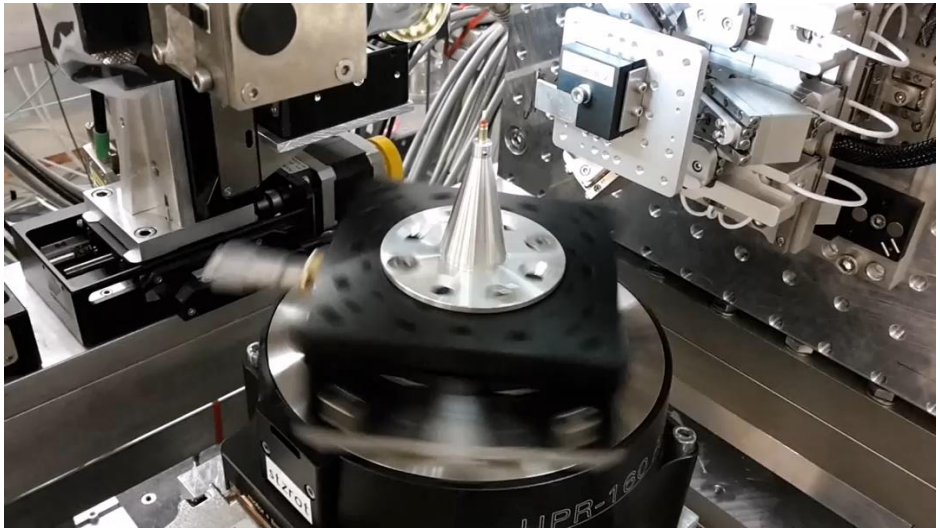

2µm SiO2 microspheres
50µm square capillary in aqueous suspension
photon energy 8keV
Fresnel number F =2.1 10^{-3}
effective pixel size px=116nm
acquisition rat 134 Hz ac. rate
rot. frequency f = 1 Hz (2 sinograms/sec)
total acquisition time 39.9 s

---

extensive data corrections, phase retrieval & tomographic reconstruction...

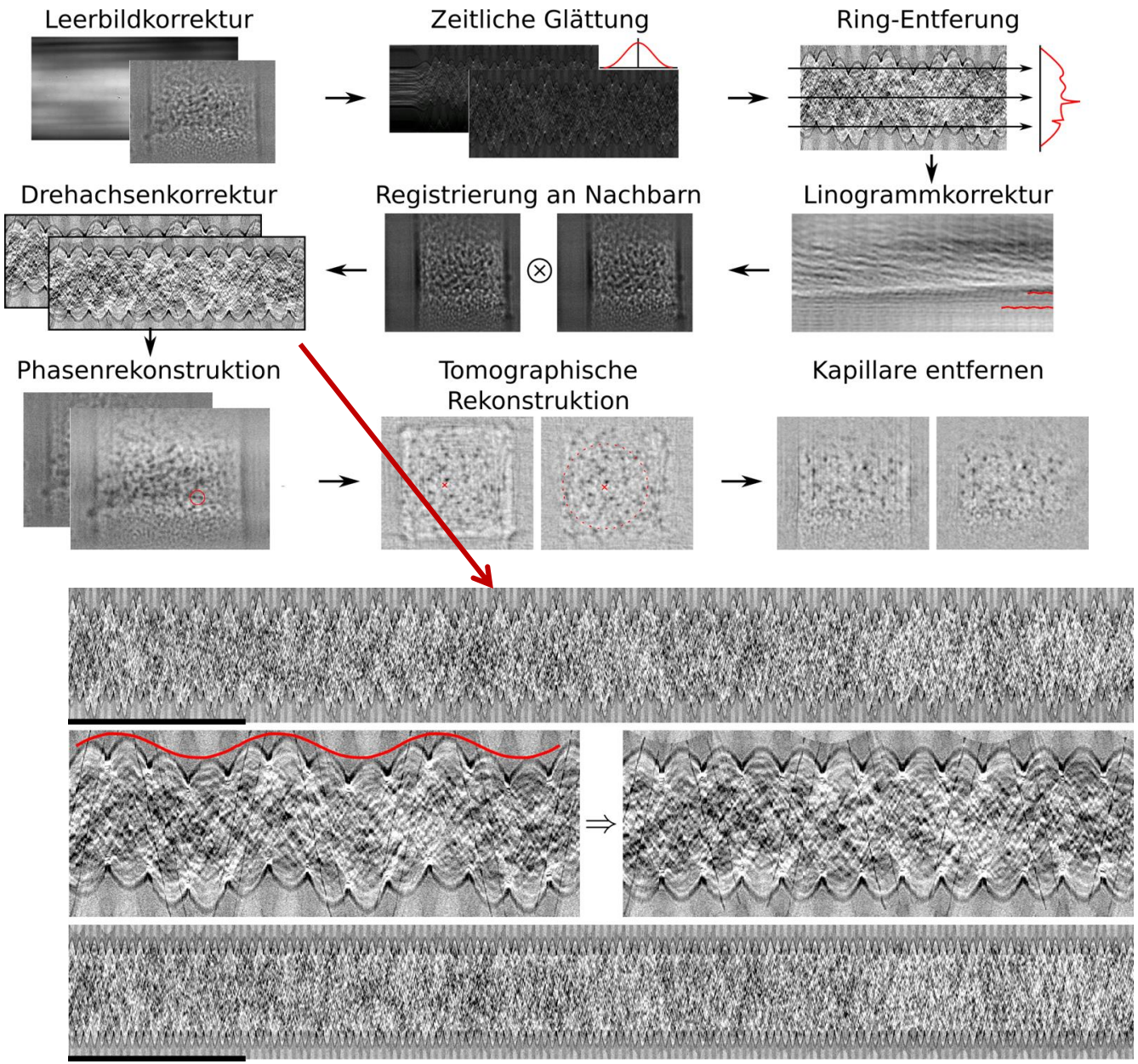

Hologramm

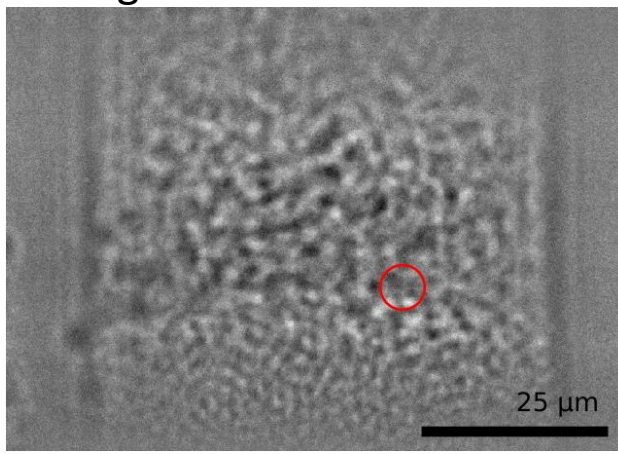

Projection (CTF-Reko.)

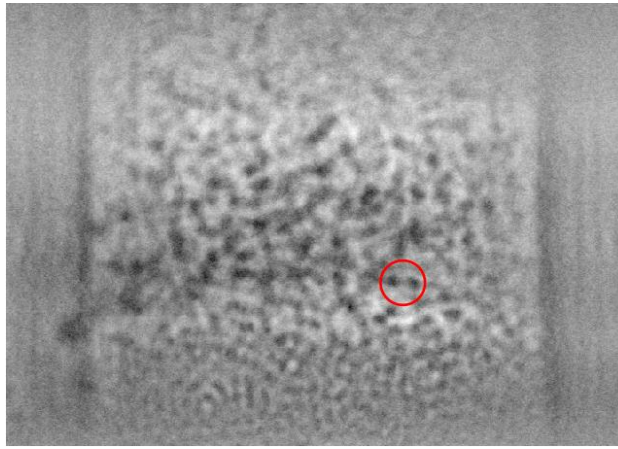

sliding window

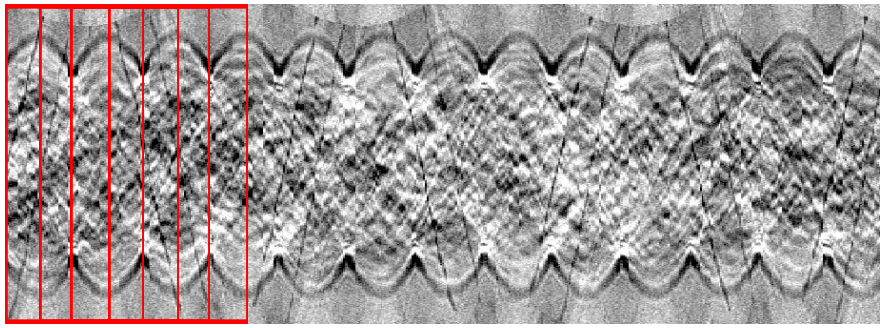

$\Delta t \approx 0.14\,\mathrm{s}$

central slice (x-z)

central slice (x-y)

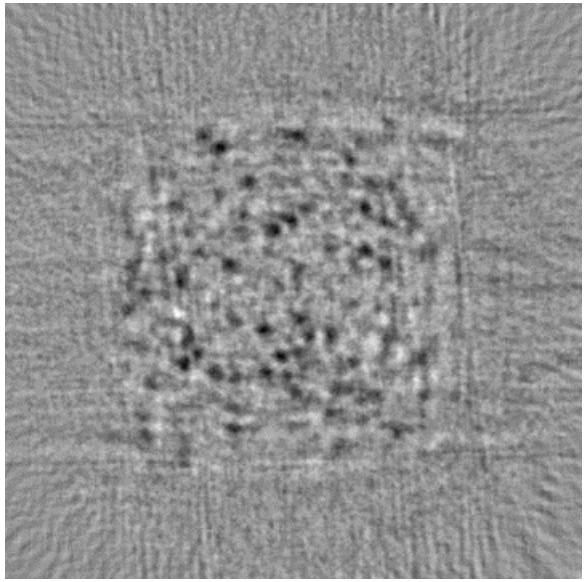

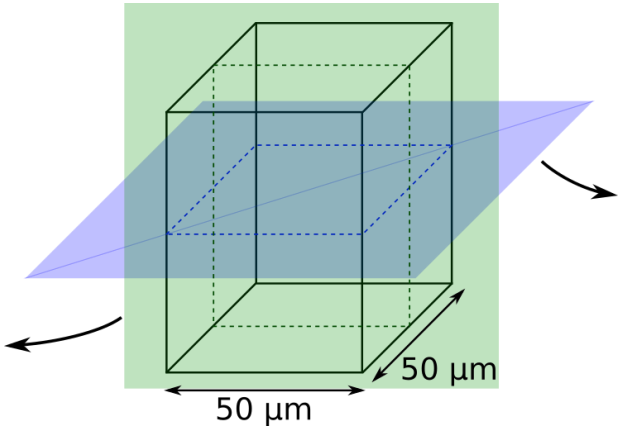

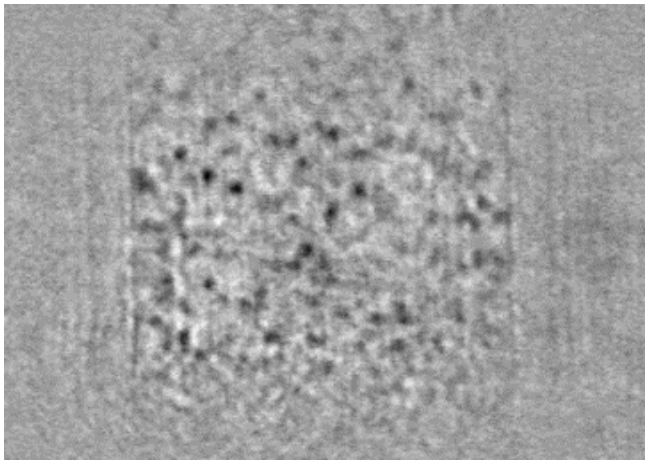

reconstruction of about 10000 trajectories (here only 1000 longest shown)

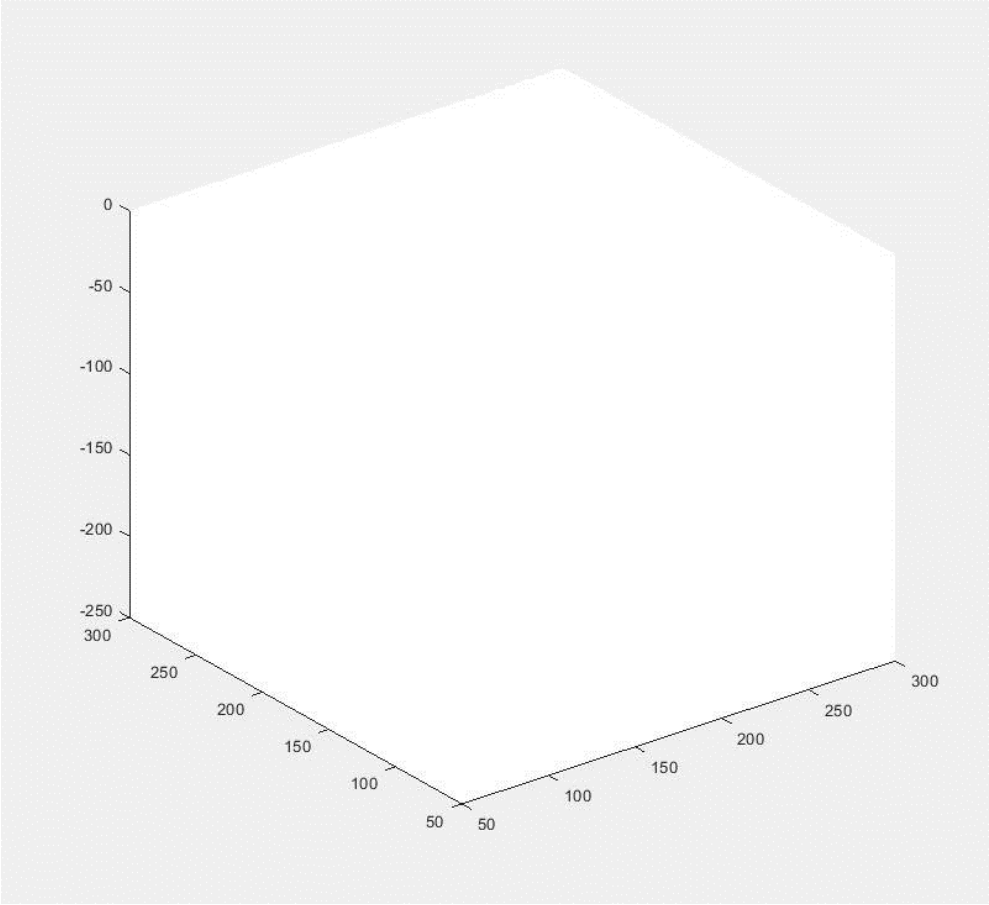

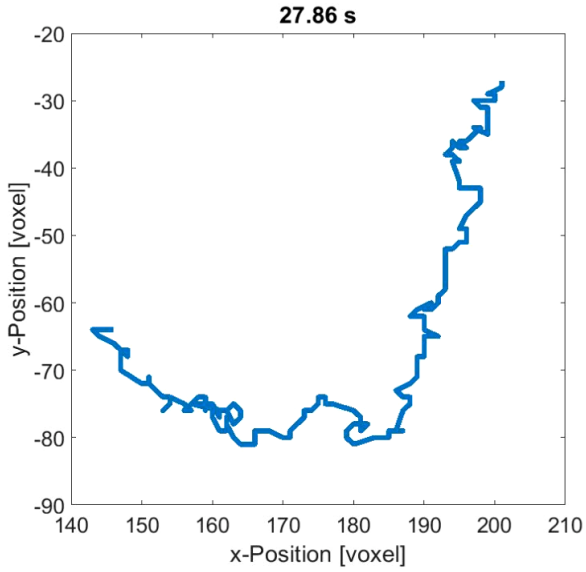

diffusion in x-z-plane

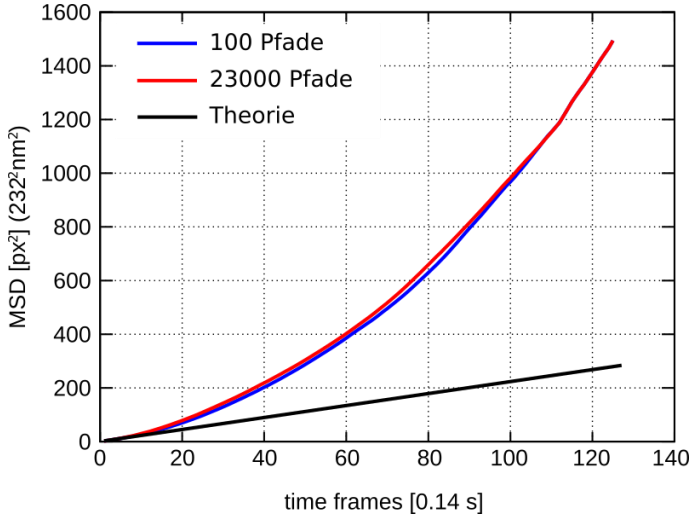








Mareike Töpperwien *tomography of neural tissues*
Aike Ruhlandt *time-resolved tomography & 3d phase retrieval*
Malte Vassholz *waveguide optics & new tomography concepts*
Martin Krenkel *tomography of cells & tissues, waveguides, lab. CT*
Mathias Bartels *high resolution waveguide imaging, live cells, cochlea CT,*
Annalena Robisch *near-field ptychography*
Aike Ruhlandt *time-resolved tomography*

Johannes Hagemann
reconstruction
beyond idealisation

Markus Osterhoff *x-ray optics, numerics, GINIX endstation*

Sarah Hoffmann, *waveguide optics and fabrication*
Hsin-Yi Chen *tapered waveguides*
Robin Wilke, *phase reconstruction algorithms, ptychography*
Marten Bernhardt cellular imaging, stem cells, nano diffraction
Marius Priebe cellular imaging, action
Jan-David Nicolas cellular imaging, actin

collaborating groups in Göttingen
Sarah Köster, Tobias Moser, Wiebke Moebius,
Frauke Alves, Reinhard Jahn, Florian Rehfeldt

DESY:
Michael Sprung, Alexey Zozulya, Eric Stellamanns,

funding:
SFB 755 Nanoscale Photonic Imaging
EXC-172 Molecular physiology of the brain
SFB 937 Collective Behavior of Soft and Biological Matter
SFB 803 Functionality by organisation of membranes…